THE JOURNAL OF PHYSICAL CHEMISTRY Letters

Perspective

pubs.acs.org/JPCL

From Conventional to Phase-Sensitive Vibrational Sum Frequency Generation Spectroscopy: Probing Water Organization at Aqueous Interfaces

Dominique Verreault, Wei Hua, and Heather C. Allen*

Department of Chemistry and Biochemistry, The Ohio State University, 100 West 18th Avenue, Columbus, Ohio 43210, United States

ABSTRACT: Elucidation of water organization at aqueous interfaces has remained a challenging problem. Conventional vibrational sum frequency generation (VSFG) spectroscopy and its most recent extension, phase-sensitive VSFG (PS-VSFG), have emerged as powerful experimental methods for unraveling structural information at various aqueous interfaces. In this Perspective, we briefly describe the two possible VSFG detection modes, and we point out features that make these methods highly suited to address questions about water organization at air/aqueous interfaces. Several important aqueous interfacial systems are discussed to illustrate the versatility of these methods. Remaining challenges and exciting prospective directions are also presented.

The ubiquitous nature of water is well reflected by the crucial role that it plays in a variety of biological, chemical, and physical processes.[1−3] A majority of these processes take place in constrained or over extended interfaces rather than in the bulk.[4−6] For example, in biochemistry, water is found closely associated to biological membranes but also embedded in internal protein cavities where it promotes ligand binding and catalysis. Similarly, in geochemistry, water is adsorbed onto mineral oxides where it contributes to ion adsorption and dissolution, as well as in capillary pores. Despite its critical importance, many features of interfacial water in these environments still remain only partly understood. It is well-known that bulk phase water exhibits many anomalous physicochemical properties,[7,8] which are related to its strong hydrogen-bonding ability. Not surprisingly, the proximity to an extended interface such as with a vapor or a condensed phase will make interfacial water also display its own peculiar behavior. The difference between interfacial and bulk water molecules in their ability to optimize hydrogen bonding will affect the organization of interfacial water and, in turn, its static and dynamic properties such as density, permittivity, and viscosity over a very short range ($\lesssim$1 nm).[9−12]

Among all extended interfaces, the air/aqueous interface has been the most intensively investigated partly due to its compositional simplicity as well as for its relevance in biophysics and atmospheric aerosol chemistry. Because of the low density of the vapor phase, weak van der Waals interactions exist between vapor and liquid phases, and consequently, only water−water interactions within the latter determine interfacial properties. Stronger hydrogen bonding between interfacial water molecules gives rise to a very high surface tension ($\gamma \approx$ 72.8 mN/m at 20 °C),[13] while the directionality of their dipole moment generates a finite surface potential ($\Delta\chi \approx +0.1-0.2$ V), whose magnitude and sign still remain highly debated.[14−16] For instance, an explicit ab initio electronic charge density study has recently suggested that a positive potential may be due to an electron density leakage into the gas phase and not to a preferential water orientation.[17] Another study has proposed instead a possible charge transfer between interfacial water molecules due to hydrogen bonding anisotropy at the water surface.[18] Another closely related topic, the surface acidity/basicity of the neat water surface resulting from the different surface propensity between hydronium and hydroxide ions, has also been strongly disputed.[19−21] Although the exact mechanism for this difference is not clearly understood, the current molecular picture based on computational and spectroscopic investigations suggests that the water surface is likely to be slightly acidic, with hydronium ions enhanced at the topmost liquid layer and hydroxide ions weakly excluded from it.[22]

Obviously, the peculiar properties of interfacial water will also influence the affinity and distribution of solvated ions as well as those of amphiphilic and nonionic solutes, thus adding to the complexity of aqueous interfaces.[23−26] For instance, it was long believed that the air/aqueous solution interface is depleted in inorganic ions because of repulsive electrostatic image charge effects and decreased ion hydration, which make ions prefer bulk solvation.[27] However, compelling evidence from both simulations and experiments on ions in water clusters and at planar air/water interfaces now supports the picture of ion adsorption in a highly specific manner, having

Received: August 13, 2012
Accepted: September 28, 2012
Published: September 29, 2012

   dx.doi.org/10.1021/jz301179g | J. Phys. Chem. Lett. 2012, 3, 3012−3028

nonpolarizable ions with high surface charge density (e.g., light alkali cations) repelled from the interface while polarizable ions with low surface charge density (e.g., heavier halide anions) show a significant surface propensity.[28−31]

MD simulations of ions in small water clusters and slabs have been particularly helpful in predicting ion surface affinity and in providing complementary theoretical guidance to experimental studies. Computational studies, based on different water and ion potential models, have identified numerous parameters potentially critical to ion surface propensity, including ion size (radius), ion surface charge density, ion and water polarizability, ion solvation structure (chaotropic versus kosmotropic),[32,33] ion−ion correlations, and so forth. It has also been suggested that interfacial curvature and fluctuations could also act as a potential driving force in ion adsorption and distribution.[34−36] Among all of these parameters, ion polarizability has emerged as crucial in determining surface affinity, at least for monovalent anions. Using polarizable force field models, it was realized early on with small water clusters[37−40] and later with planar aqueous interfaces[41,42] that when polarization effects are included, large polarizable ions prefer residing at the interface. This ion-specific affinity has been explained as originating from favorable interactions that exist between the polarizability of an ion and the surface electric field induced by the average orientation of interfacial water molecules. This interpretation has also been predicted by a recent theoretical partitioning model.[43] Finally, in parallel to MD simulations, different theoretical models have also attempted to identify other possible driving forces at the origin of ion adsorption at the neat air/water interface.[44,45]

In agreement with simulations, the application of novel surface spectroscopic techniques such as electrospray mass ionization (EMI) spectrometry,[46] glancing-angle Raman spectroscopy,[47,48] IR photodissociation spectroscopy,[49,50] grazing incidence X-ray fluorescence (GIXF),[51] and high-pressure X-ray photoelectron spectroscopy (HP-XPS)[52] has enabled researchers to probe the interfacial region of aqueous solutions with varying degrees of sensitivity. In particular, HP-XPS measurements performed on aqueous liquid microjets have provided strong evidence for ion enhancement by measuring directly ion interfacial concentrations. However, as with other electron-based spectroscopies, experiments using this technique must be performed under an evacuated environment, albeit at higher pressure than typical XPS, a limitation in regards to its applicability to aqueous solutions.

Another type of a highly surface sensitive technique, namely, second-order nonlinear spectroscopies such as vibrational sum frequency generation (VSFG) and surface second-harmonic generation (SHG), has also proven increasingly useful in providing information about ion surface affinity at aqueous interfaces.[30,53−57] Their decisive advantage lies in their selection rules that result in the suppression of the bulk response, which makes them highly surface specific (∼1−5 nm). Furthermore, these have shown to have submonolayer sensitivity, to be noninvasive, and applicable in situ (i.e., under ambient conditions) provided that the interface can be accessed by light. It has been possible with UV SHG measurements to determine ion affinity (i.e., Gibbs free energy adsorption) by using the SHG response of the ion charge-transfer-to-solvent (CTTS) resonance together with adsorption models as a function of bulk ion concentration.[58,59] In contrast, conventional VSFG measurements performed on aqueous solutions have mostly focused on the perturbations of the water hydrogen-bonding network induced by the surface electrostatic field in the electric double layer (EDL) as an indirect probe of ion surface affinity; so far, very few studies have directly probed ions or chemical groups of more complex solutes.[60−62]

Recently, phase-resolved or phase-sensitive (PS)-VSFG has allowed determination of the absolute orientation of interfacial water molecules and indirect deduction of the direction of the surface field in the EDL, thereby giving an idea of the relative ion surface propensities.[63,64] Despite their high surface sensitivity, it still remains difficult to extract interfacial ion concentrations based solely on a molecular-level interpretation of the perturbed water spectra. Hence, taking into account the nature of water hydrogen bonding, the inherent complexity of aqueous interfaces, as well as the limitations of current computational and experimental methods, it appears clear that a comprehensive understanding of interfacial water organization as well as its perturbation by solvated and/or complexed solutes presents a formidable challenge. The predictive ability of computational models is limited at reproducing accurately experimental spectra, while molecular interpretation of experimental spectra remains often not trivial, such that quantitative discrepancies always subsist between simulations and experiments. Nevertheless, substantial progress has been made in the past decade with both the continuous improvement of MD simulations and the development of novel experimental surface-sensitive techniques.

Taking into account the nature of water hydrogen bonding, the inherent complexity of aqueous interfaces, as well as the limitations of current computational and experimental methods, it appears clear that a comprehensive understanding of interfacial water organization as well as its perturbation by solvated and/or complexed solutes presents a formidable challenge.

This Perspective reviews some recent advances made with conventional VSFG and newly developed PS-VSFG spectroscopy in elucidating interfacial water organization as well as ion affinity to various aqueous interfaces. Specific examples from our most recent published work at the air/aqueous and lipid/aqueous interfaces as well as some complementary computational and experimental contributions from others are given to illustrate the usefulness and wide application of both techniques. Motivation in the choice of these aqueous interfaces mainly comes from the relevance of these unique environments (e.g., aerosols, biomembranes, minerals) and the reactions that they host in atmospheric chemistry, biochemistry, and geochemistry.

Conventional and Phase-Sensitive VSFG Spectroscopy. Infrared (IR)−visible (VIS) VSFG spectroscopy, referred hereafter as conventional VSFG, and PS-VSFG spectroscopy have become invaluable techniques well-suited for probing the structure (ordering, orientation) of various interfaces at the molecular level. The physical basis of these techniques lies in sum

frequency generation (SFG), a second-order nonlinear optical (two-photon) process by which spatial and temporal mixing of two input beams at frequencies ω_1 and ω_2 in a non-centrosymmetric medium ($\chi^{(2)} \neq 0$, where $\chi^{(2)}$ is the medium second-order nonlinear susceptibility) generates a coherent output beam at the sum frequency (SF) $\omega_3 = \omega_1 + \omega_2$. Under the electric dipole approximation, this process is forbidden in the bulk of centrosymmetric media ($\chi^{(2)} = 0$), typical of most materials.[65,66] However, at the interface between two such media, the symmetry is naturally broken, and the SFG process is allowed. This lack of interfacial inversion symmetry becomes a unique selection rule that confers to these techniques their high surface specificity.

Infrared–visible VSFG spectroscopy and PS-VSFG spectroscopy have become invaluable techniques well-suited for probing the structure of various interfaces at the molecular level.

On the basis of this selection rule, it was first demonstrated in 1987 by Shen and co-workers[67−69] that SFG can be used as a surface-specific tool for spectroscopic interrogation of various interfaces. Hence, conventional VSFG spectroscopy enables one to probe the vibrational properties of interfacial species by overlapping spatially and temporally two intense pulsed laser beams, one tunable in the IR frequency ($\omega_1 = \omega_{IR}$) range and another fixed at a visible (or near-IR) frequency ($\omega_2 = \omega_{VIS}$) (Figure 1A). The vibrational modes are interrogated by the resonant IR beam and upconverted by the nonresonant VIS beam into the visible spectral region through a virtual state, from which an emitted SF beam can be detected. Whenever the IR frequency matches the energy of an interfacial vibrational transition, the VSFG signal is resonantly enhanced. Hence, recording the intensity of this signal as a function of the IR frequency gives access to the vibrational spectrum of interfacial species. The intensity of the generated SF signal in the reflected direction is proportional to the squared modulus of the effective second-order nonlinear susceptibility $\chi^{(2)}_{eff}$ as well as to the intensities of IR (I_{IR}) and VIS (I_{VIS}) input beams[70]

$$I_{VSFG}(\omega_{IR}) \propto |\chi^{(2)}_{eff}(\omega_{IR})|^2 I_{IR} I_{VIS} \tag{1}$$

with

$$\chi^{(2)}_{eff}(\omega_{IR}) = [\hat{\mathbf{e}}_{SF}\cdot\mathbf{L}_{SF}]\cdot\chi^{(2)}_{S}(\omega_{IR}):[\mathbf{L}_{IR}\cdot\hat{\mathbf{e}}_{IR}][\mathbf{L}_{VIS}\cdot\hat{\mathbf{e}}_{VIS}] \tag{2}$$

where $\chi^{(2)}_S$ is the (macroscopic) second-order surface nonlinear susceptibility, while $\hat{\mathbf{e}}_i \equiv \hat{\mathbf{e}}(\omega_i)$ and $\mathbf{L}_i \equiv \mathbf{L}(\omega_i)$ refer to the unit polarization vector and the transmission Fresnel factor at frequency ω_i (i = SF, IR, VIS), respectively.

The magnitude of $\chi^{(2)}_S$ is related to the microscopic hyperpolarizability $\beta^{(2)}$ through

$$\chi^{(2)}_S = N\langle\beta^{(2)}\rangle \tag{3}$$

with $\beta^{(2)}$ given by the product of the Raman transition polarizability moment (α) and the IR transition dipole moment (μ)

$$\beta^{(2)} = \langle g|\alpha|\nu\rangle\langle\nu|\mu|g\rangle \tag{4}$$

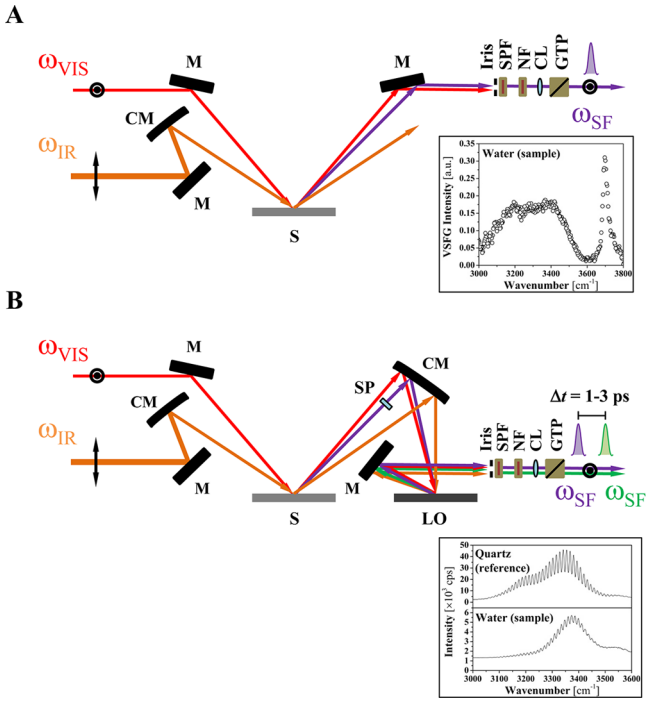

Figure 1. Schematic representation of VSFG measuring schemes and examples of spectra from the air/water interface. (A) Conventional VSFG spectroscopy and (B) PS-VSFG spectroscopy. The optical components are as follow: CL, convex lens; CM, concave mirror; GTP, Glan–Thompson polarizer; LO, local oscillator; M, mirror; NF, notch filter; S, sample; SPF, short-pass filter.

where N is the number of molecules contributing to the SF signal and g and ν are the ground and excited vibrational states, respectively. The angular brackets denote the orientational averaging. Taken together, eqs 3 and 4 basically state that in order to generate an SF signal, a vibrational transition must be both IR- and Raman-active and that this signal can be enhanced either by (i) a greater alignment ($\langle\beta^{(2)}\rangle$) of molecular transition dipole moments along the surface normal or by (ii) a larger number (N) of ordered (or oriented) molecules.

For discrete vibrational modes, $\chi^{(2)}_S$ can be expressed as

$$\chi^{(2)}_S(\omega_{IR}) = \chi^{(2)}_{NR} + \sum_k \chi^{(2)}_{R,k}(\omega_{IR}) = \chi^{(2)}_{NR} + \sum_k \frac{A_k}{(\omega_{IR} - \omega_k) + i\Gamma_k} \tag{5}$$

where $\chi^{(2)}_{NR}$ and $\chi^{(2)}_{R,k}$ denote the nonresonant and resonant contributions to $\chi^{(2)}_S$, respectively. The resonant contribution can be modeled as a sum of Lorentzian-like functions, each characterized by an amplitude A_k, a central frequency ω_k, and a (homogeneous) transition line width (fwhm) Γ_k. The amplitude of the SF transition moment in eq 5 is proportional to the product of the orientation-averaged IR transition dipole and Raman transition polarizability moments (eq 4). Other more general functions such as Voigt-like distribution functions can also be assumed when one also takes into account inhomogeneous broadening due to the different molecular environments.[71] More generally, for continuous modes (e.g., collective OH vibrational modes of interfacial water), the summation in eq 5 is replaced by an integration over the density of modes $\rho(\omega_k)$ at frequency ω_k.

dx.doi.org/10.1021/jz301179g | J. Phys. Chem. Lett. 2012, 3, 3012−3028

In conventional VSFG spectroscopy, all of the molecular information is folded in the factor $|\chi_S^{(2)}(\omega_{IR})|^2$, where $\chi_S^{(2)}$ is complex and can be put in the form (with $\chi_{NR}^{(2)}$ being constant)

$$\chi_S^{(2)}(\omega_{IR}) = |\chi_S^{(2)}|e^{i\phi_S(\omega_{IR})} = \mathrm{Re}\,\chi_S^{(2)} + i\,\mathrm{Im}\,\chi_S^{(2)} \quad (6)$$

where $|\chi_S^{(2)}|$ and ϕ_S are the amplitude (modulus) and phase of $\chi_S^{(2)}$, respectively. Following eq 5, the imaginary part of $\chi_S^{(2)}$ then takes the form

$$\mathrm{Im}\,\chi_S^{(2)} = -\sum_k \frac{A_k\Gamma_k}{(\omega_{IR} - \omega_k)^2 + \Gamma_k^2} \quad (7)$$

Clearly, from eqs 1 and 6, the VSFG response contains information on both the amplitude and the phase (orientation) of the VSFG transition moment and, in turn, on the orientation of the induced dipole moment. However, accessing this information through conventional VSFG spectroscopy presents two drawbacks. First, $|\chi_S^{(2)}(\omega_{IR})|^2$ needs to be extracted from the VSFG intensity by correcting for the Fresnel factors that account for the specific setup geometry (incident beam angles and polarizations, refractive indices of the media). In previous studies, this procedure has either not been explicitly mentioned or simply disregarded and has led, for instance in the case of the air/water interface, to some inconsistencies when comparing VSFG spectra. However, this issue has been recently discussed, and a standardization has been called for.[72] Second, and more importantly, because of the conventional VSFG spectroscopy detection scheme (see eq 1), it becomes impossible to directly measure the phase information contained in $\chi_S^{(2)}$. In principle, for discrete resonances, it is possible to obtain the phase information through fitting of the experimental data, but without fixing beforehand the frequencies and signs of the vibrational modes, it comes down to selecting between nonunique sets of fittings parameters.[73] This has led, for example, to different and often contradictory structural interpretations of the VSFG spectra of the air/water interface.

More recently, these limitations of conventional VSFG spectroscopy have been alleviated by novel computational and experimental methods enabling determination of the phase information. Phase retrieval algorithms based on the maximum entropy method (MEM) were developed by Bonn and co-workers to reconstruct the absolute phase of the SF signal directly from VSFG intensity spectra.[74] This approach has proven successful with many aqueous interfaces, and $\mathrm{Im}\,\chi^{(2)}$ complex spectra were shown to follow closely with those obtained by direct phase measurement.[75,76] Nevertheless, the phase retrieval method suffers from a certain number of weaknesses that are at the origin of the discrepancies between reconstructed and directly measured phase spectra such as phase shifting (error phase), complex conjugation sign convention, and dependence on the VSFG spectra S/N ratio.[76] For example, for systems with large nonresonant phases (e.g., self-assembled monolayers of alkanethiols on gold), supplementary information such as the sign of the nonresonant phase or some previous information on the molecular arrangement (orientation) is typically required to retrieve the correct phase of any given vibrational mode. Without such an a priori knowledge, the phase retrieval procedure cannot select the correct fit and, therefore, determine the absolute phase.

The inability of conventional VSFG spectroscopy to directly measure the phase was recognized shortly after its first application. In fact, as early as 1990, Shen and co-workers were able to measured the phase of a pentadecanoic acid monolayer on water with VSFG.[77,78] However, the technique received little attention, partly due to the added instrumental complexity. Many years later, PS-VSFG was demonstrated on scanning SFG systems by the same group and applied to probe interfaces between centrosymmetric and noncentrosymmetric media (e.g., quartz/water interface)[79] as well as between centrosymmetric media.[80] It was later extended to broad bandwidth SFG systems by Benderskii's and Tahara's groups.[81−83]

PS-VSFG spectroscopy is an interference-based version of conventional VSFG spectroscopy by which the VSFG signal from a sample (S) is mixed with an additional signal called local oscillator (LO) generated from a known nonresonant medium (e.g., GaAs(110)), which enables absolute determination of the sign of $\chi_S^{(2)}$ and ultimately provides the orientation of SF transition dipole moments of interfacial species. Like in conventional VSFG spectroscopy, the IR and VIS beams are spatially and temporally overlapped on a sample surface (Figure 1B). However, the SF beam generated in the reflection direction is time-delayed relative to the IR and VIS beams by passage through a silica plate, before all three beams become refocused onto the LO medium. The spatial and temporal overlap of the refocused IR and VIS beams then generates another SF beam. The two generated SF beams (from the sample and LO medium) are finally separated in time and mixed to give an interference pattern in the frequency domain. The detected total intensity is thus the sum of the SF electric fields from the sample (E_S) and LO (E_{LO}) medium and is given by[83]

$$\begin{aligned} I_{PS\text{-}VSFG} &= |r_{LO}E_S e^{i\omega\Delta t} + E_{LO}|^2 \\ &= |r_{LO}E_S|^2 + |E_{LO}|^2 \\ &\quad + r_{LO}^* E_S^* E_{LO} e^{-i\omega\Delta t} + r_{LO}E_S E_{LO}^* e^{i\omega\Delta t} \end{aligned} \quad (8)$$

with[84]

$$E_S \propto \chi_S^{(2)} E_{VIS} E_{IR} \quad (9a)$$

$$E_{LO} \propto \chi_{LO}^{(2)} r_S(\omega_{VIS}) r_S(\omega_{IR}) E_{VIS} E_{IR} \quad (9b)$$

where Δt denotes the time delay between the two SF beams, whereas r_S and r_{LO} are the complex Fresnel reflection coefficients that take into account the reflection off of the sample and the LO medium.

As readily seen from eq 8, the main advantage of PS-VSFG spectroscopy comes from the fact that by using the interference between two sources (sample and LO), cross terms of the intensity are generated in which phase information is preserved. In order to extract $\chi_S^{(2)}$, the fourth term of eq 8 must be extracted. To this end, the different terms in eq 8 are time-separated by inverse Fourier transformation into the time domain, and then the quadratic and negatively time-delayed terms at $t = 0$ and $-\Delta t$, respectively, are filtered out, and the remaining term is Fourier-transformed back into the frequency domain.[83,84] Finally, the resulting complex frequency spectra that contain the sample phase information are normalized to the reflectivities of IR and VIS beams on a frequency-independent reference ($\chi_S^{(2)}$ constant). For instance, a z-cut quartz crystal has no resonance in the water spectral region such that its phase can be used as a reference. The normalized PS-VSFG intensity is then given by[84]

dx.doi.org/10.1021/jz301179g | J. Phys. Chem. Lett. 2012, 3, 3012−3028

$$I_{\text{PS-VSFG}} = \frac{E^*_{\text{LO,S}}E_{\text{S}}}{e^{i\Delta\phi}E^*_{\text{LO,R}}E_{\text{R}}} = \frac{F_{\text{S}}}{F_{\text{R}}}\left(\frac{r_{\text{S}}(\omega_{\text{VIS}})r_{\text{S}}(\omega_{\text{IR}})}{r_{\text{R}}(\omega_{\text{VIS}})r_{\text{R}}(\omega_{\text{IR}})}\right)^* \frac{\chi^{(2)}_{\text{S}}}{\chi^{(2)}_{\text{R}}} \tag{10}$$

where F_{R} and F_{S} refer to the Fresnel factors of the reference and sample and where $\Delta\phi$ accounts for the phase difference between the SFG response of the sample and that of the reference. For example, it has been theoretically predicted that the surface SFG response of aqueous interfaces and the bulk response of quartz should exhibit a phase difference of 90°;[85] however, this value has been recently contested.[72,86]

Using eq 6, the normalized $\text{Im}\,\bar{\chi}^{(2)}_{\text{S}}$ immediately follows

$$\text{Im}\,\bar{\chi}^{(2)}_{\text{S}} = \left|\frac{F_{\text{R}}}{F_{\text{S}}}\left(\frac{r_{\text{R}}(\omega_{\text{VIS}})r_{\text{R}}(\omega_{\text{IR}})}{r_{\text{S}}(\omega_{\text{VIS}})r_{\text{S}}(\omega_{\text{IR}})}\right)\right|\left|\frac{E^*_{\text{LO,S}}E_{\text{S}}}{E^*_{\text{LO,R}}E_{\text{R}}}\right| \times \sin(\phi_{\text{S}} - \phi_{\text{R}}) \tag{11}$$

Hence, eq 11 contains information on the phase ϕ_{S} of the sample that, in turn, determines the sign of $\text{Im}\,\chi^{(2)}_{\text{S}}$ and enables a distinction between interfacial molecules oriented downward and upward at the interface. Despite its decisive advantage over conventional VSFG, PS-VSFG spectroscopy still has to deal with some important challenges, among which are the yet unexplained additional phase from the crystal quartz reference, the lack of consistency in the application of phase corrections (e.g., taking into account the sample's complex reflection coefficient) and in the reconstruction of the power spectrum from the real and imaginary parts ($|\chi^{(2)}_{\text{S}}|^2$), the control of the phase instability common to phase-resolved experimental setups, and the discrepancies between the water phase spectra between different research groups[83,93] (e.g., variations in the spectral location of the zero crossing point, in the amplitude ratio between lower and higher frequency regions, and in the overall shape) or even within the same group (compare for example, Figures 2C and 5B in the present text).[72,84] Clearly, there are analytical and experimental difficulties that need to be addressed, but the general trends are reproducible. With the wider implementation of the phase detection mode and adoption of accepted data correction procedures in a manner similar to conventional VSFG spectroscopy, it is expected that PS-VSFG spectroscopy will also mature over the next few years.

With the wider implementation of the phase detection mode and adoption of accepted data correction procedures in a manner similar to conventional VSFG spectroscopy, it is expected that PS-VSFG spectroscopy will also mature over the next few years.

Air/Water Interface. The neat air (vapor)/water interface, undoubtedly the most studied of all aqueous interfaces, has always attracted much attention because of its relative (compositional) simplicity, its unique place as a control for other aqueous interfaces, and finally, its prevalence in numerous atmospheric, biophysical, geochemical, as well as industrial processes.[87] In fact, it is generally recognized that only the topmost few layers of water molecules, structurally different than the bulk, regulate the reactivity and functionality of most

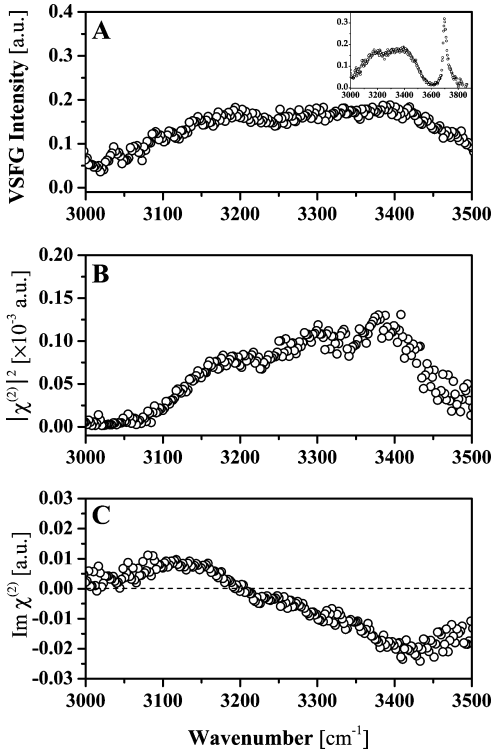

Figure 2. ssp-Polarized conventional VSFG spectrum (A), deduced power spectrum (B), and PS-VSFG spectrum (C) of the neat air/water interface in the hydrogen-bonded OH stretching region. The inset in the top panel depicts the whole conventional VSFG water spectrum including the dangling OH region. The weaker intensity on the flanks of the power spectrum as opposed to that of the conventional VSFG spectrum is due to the lower IR energy, which is below the SFG conversion threshold in the phase detection mode (adapted from ref 161).

of these processes. Hence, an accurate description of water organization at the air/water interface is necessary to understand the interplay between interfacial water molecules and dissolved or adsorbed solutes (e.g., ions, lipids, proteins, macromolecular assemblies, etc.) and, ultimately, its role in controlling the whole interfacial chemistry.

A molecular picture of interfacial water organization and its perturbation by solutes can be generally deduced from its vibrational spectrum, which probes the coordination and cooperativity of water's hydrogen-bonding network at the interface.[30,88−91] As mentioned above, this can be accomplished by means of surface-specific nonlinear spectroscopic techniques such as conventional VSFG spectroscopy. Because of its inherent surface specificity due to the noncentrosymmetry selection rule, conventional VSFG spectroscopy probes a very thin region of the neat water surface, typically equivalent to ∼2−3 water layers. Furthermore, as indicated by eq 3, the SF response will reflect the amount of coordination and the strength of cooperative interactions in each of these layers. The first VSFG intensity spectrum of the neat air/water interface was reported by Shen and co-workers as early as 1993[92] and has since been repeatedly reproduced by other groups with relative consistency.[72] A typical conventional VSFG spectrum of the OH stretching modes from the neat air/water interface spans a large spectral region from 3000 to 3800 cm^{-1}, which is indicative of interfacial water species in different local hydrogen-bonding environments (Figure 2A). It basically

dx.doi.org/10.1021/jz301179g | J. Phys. Chem. Lett. 2012, 3, 3012−3028

consists of a very broad band ranging from 3000 to ~3600 cm^{-1} and a narrow band centered at around 3700 cm^{-1}. The narrow band is typically assigned to the dangling OH stretching of topmost surface water molecules with the OH bond protruding into the vapor phase. The broad water band is generally attributed to the collective OH stretching modes of hydrogen-bonded water molecules located in the subsurface layers (a few Å away from the top surface layer) that display additional coordination and higher cooperativity; traditionally, this spectral region has been deconvolved into two discrete subbands located at around 3200 and 3450 cm^{-1}, either with opposite (+,−) or similar (−,−) phases. Two possible but radically different molecular interpretations have been proposed for this region, including, on one hand, the variation of hydrogen-bonding geometry and strength of interfacial molecules with their neighbors[93] and, on the other hand, the intramolecular coupling (or Fermi resonance) between the symmetric OH stretching and bending overtone.[94] Moreover, following the latter interpretation, it was subsequently argued that another (positive) lower-frequency (~3100 cm^{-1}) band should be added in order to be fully consistent with both $|\chi_S^{(2)}|^2$ and $\mathrm{Im}\,\chi_S^{(2)}$ spectra.[95] However, no molecular origins have been furnished for this band. Thus, a definite assignment of the origin and uniqueness of these bands still remains debated. In recent years, several other spectral analyses based on three resonances have been reported, leading to different structural interpretation as to which interfacial water species contribute to which part of the bound OH region.[96]

As mentioned previously, PS-VSFG spectroscopy can also provide additional information on the net orientation of water molecules in the interfacial water region. Despite similar $|\chi_S^{(2)}|^2$ spectra (Figure 2B), earlier $\mathrm{Im}\,\chi_S^{(2)}$ spectra obtained through fitting all showed poor reproducibility, especially in the bonded OH stretching region, with varying negative amplitudes for both the ~3200 and ~3400 cm^{-1} bands, suggesting hydrogen-bonded water species mostly oriented toward the liquid phase. In contrast, the first experimental PS-VSFG spectrum, also obtained by Shen and co-workers,[93] typically showed for the bonded OH region a positive band at lower frequency (≤3200 cm^{-1}) and a negative band at higher frequency (3200−3600 cm^{-1}), along with a positive band for the dangling OH band. The positive and negative bands in the bonded OH region correspond mainly to water species with their OH bonds directed toward the bulk gaseous and liquid phases, respectively, although the interpretation is still somewhat debated.[97,98] In comparison to the $\mathrm{Im}\,\chi_S^{(2)}$ spectra obtained through fitting, the experimental ones show a marked difference, particularly below 3200 cm^{-1}, where the amplitude is now positive (Figure 2C).[99,100] It was argued that the discrepancy arises from the choice of discrete vibrational modes instead of a continuous modal distribution.[96]

Even though conventional and, more recently, PS-VSFG spectroscopy have furthered the molecular-level understanding of the neat water surface in terms of the coordination, strength, and orientation of water molecules within the hydrogen-bonding network, theoretical modeling of the spectral data is still necessary to predict the contribution of the different interfacial water species to the various spectral regions. Unfortunately, despite recent advances, MD simulations of the neat air/water interface have so far been partially successful in accurately reproducing experimental data and, in turn, at providing a definite and unambiguous molecular interpretation of the neat water spectra.[97,98,101−113] As such, VSFG spectroscopy together with computational studies has yet to decipher basic phenomena such as the surface acidity/basicity of neat water.

Ions at the Air/Water Interface. Not surprisingly, the adsorption of solvated inorganic ions at the air/water interface has also sparked great interest, particularly in atmospheric and oceanic chemistry, because these are involved in a variety of important heterogeneous reactions in processes ranging from acid rain production through cloud and ice nucleation to ozone depletion and production.[23,29,114,115] For example, autocatalytic oxidation of halide ions (Br^-, Cl^-, I^-) at the sea salt/aqueous interface releases reactive halogen species (e.g., Br_2, BrCl) into the atmosphere, which contributes to tropospheric ozone depletion in polar regions.[116−118] Another such reaction involves gas-phase ozone with bromide and chloride ions in the remote marine boundary layer, resulting in the production of reactive halogen species, which has also implications for tropospheric ozone and hydrocarbons concentrations as well as for cloud condensation nuclei.[119,120] Heterogeneous chemical reactions like these will thus depend strongly on the availability and, in the case of acids, on the dissociation of reacting species in the interfacial region.

The effect of solutes on the VSFG spectra of aqueous solutions can be deduced by taking the neat air/water interface as a reference. In this manner, water serves as an indirect probe to study the impact of the ions on the local water environment, the direction of the surface electrostatic field generated by the EDL can be found, and the partitioning of different ions can be deduced.

Although the subsurface distribution of anions and cations has been predicted by MD simulations,[41,42] it was only recently that experimental evidence was provided supporting the picture of an EDL spontaneously formed at the air/aqueous solution interface.[63,64] This EDL usually (but not always) originates from the partition between larger, more polarizable monovalent anions, closer to the surface, and less polarizable cations repelled from it. The presence of this ion distribution at or near an interface can thus affect the water VSFG spectrum in two possible ways, (1) reorientation of water molecules responding to the surface electrostatic field created by the EDL and (2) disruption of the water hydrogen-bonding network. As in the case of the air/water interface, conventional VSFG spectroscopy can monitor any of these structural changes in the interfacial water organization by probing spectral changes in the OH stretching region resulting from the presence of an EDL at the interface. In other words, the effect of solutes on the VSFG spectra of aqueous solutions can be deduced by taking the neat air/water interface as a reference. In this manner, water serves as an indirect probe to study the impact of the ions on the local water environment. In addition, because PS-VSFG enables one to determine the absolute orientation of different OH species, it can help to find the direction of the surface electrostatic field

generated by the EDL. Finally, depending on the magnitude of the $\mathrm{Im}\,\chi_S^{(2)}$ spectrum that reflects the ion screening effect, the partitioning of different ions can be deduced. The information regarding the relative distribution of anions versus cations has been a particularly exciting outcome of PS-VSFG studies.

Because of their importance in atmospheric aerosols chemistry, early studies with conventional VSFG spectroscopy have primarily focused on the impact on interfacial water ordering from acidic solutions of halide ions (Cl^-, Br^-, I^-) as well as their aqueous salt solutions with either mono- or divalent counterions (e.g., Na^+, Mg^{2+}, Ca^{2+}).[99,121−127] For acidic solutions, VSFG spectra revealed a significant disruption of the neat air/water interface with an intensity increase in both low and high frequency hydrogen-bonded OH stretching regions (~3200 and ~3450 cm^{-1}) but a decrease in the dangling OH stretching region (~3700 cm^{-1}) (Figure 3). The

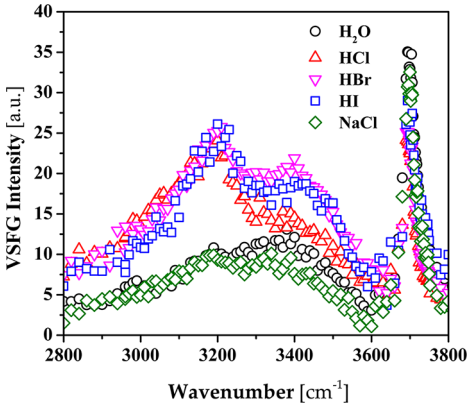

Figure 3. ssp-Polarized conventional VSFG spectra in the OH stretching region of neat water and alkali halide salt solutions. All solutions had a concentration of 1.2 M (adapted from ref 127).

signal enhancement in the hydrogen-bonded OH stretching region was attributed to an interfacial enrichment in hydrated hydronium (H_3O^+ and/or $H_5O_2^+$) ions and very polarizable anions (Br^-, I^-), respectively.[127] The spectral changes were also observed to increase with increasing anion size, polarizability, and concentration. It was suggested that these hydrated ions can influence the water VSFG spectra either by their own presence or by generation of a surface electrostatic field, which aligns interfacial water molecules and, in turn, increases interfacial depth and ordering relative to that of neat water. In contrast, in the case of basic solutions (e.g., NaOH), VSFG spectra exhibit only a weak decrease over the whole hydrogen-bonded OH stretching region.[99,126] This has been attributed to the randomization by OH^- ions of water molecules in the interfacial region.[126] The dangling OH remains practically unaltered, possibly suggesting that the influence of OH^- ions does not extend to the topmost water layer. Overall, even though a measure of hydronium or hydroxide ion concentrations at the neat water surface by VSFG spectroscopy is experimentally challenging because of the SF signal convolution with water OH stretching modes, it does suggest indirectly that the neat water surface is more likely to be slightly more acidic with hydronium ions showing more surface propensity than hydroxide ions.

Recently, results obtained by PS-VSFG spectroscopy have added more insight into this molecular picture.[99] In comparison to neat water, the $\mathrm{Im}\,\chi_S^{(2)}$ spectra of HCl and HI solutions exhibited mostly changes in the bonded OH region with greater negative amplitude, including a change of sign in the region below ~3200 cm^{-1}. This enhancement was attributed to the EDL formed between preferentially adsorbed H_3O^+ ions and polarizable anions, which creates an excess positive electrostatic field. The sign inversion of $\mathrm{Im}\,\chi_S^{(2)}$ is mainly due to orientation of the trigonal H_3O^+ ions with their O−H bonds directed toward the liquid phase. These findings have also been supported by various MD simulations.[128,129] As for the $\mathrm{Im}\,\chi_S^{(2)}$ spectrum of the NaOH solution, it shows negative amplitude between 3200 and 3500 cm^{-1}, although smaller than that for neat water, and a nearly vanishing signal below 3200 cm^{-1}. These spectral features have been interpreted as being caused, on one hand, by the reorientation of water molecules (with their O−H bonds directed toward the gaseous phase) due to the weak surface field induced by an interfacial excess of OH^- ions and, on the other hand, by the replacement of subsurface strongly hydrogen-bonded water species and/or the incorporation of OH^- ions in the hydrogen-bonding network. However, this interpretation is at odds with previous ones deduced from conventional VSFG spectra (see above) and also with MD simulations that predict that OH^- should be repelled from the water surface.[128,129] As mentioned previously, partly due to the lack of adequate theoretical models reproducing these spectral features, it not yet clear why H_3O^+ and OH^- ions, which are both influential on the hydrogen-bonding network (H_3O^+ being a good triple donor and poor acceptor and OH^- being a quadruple acceptor and a poor donor), should be preferentially adsorbed or excluded from the interface, respectively,[22] and also how the incorporation of these ions in the hydrogen-bonding framework should be related to the conventional and phase spectra.[99]

Similarly, conventional VSFG spectroscopy of alkali halide salt solutions (e.g., NaF, NaCl, NaBr, and NaI) has shown that the water's hydrogen bonding is also affected by the presence of salts, albeit to a lesser extent than the hydrogen halide solutions.[123,124] The intensity of the hydrogen-bonded OH region at around 3250 cm^{-1} decreased with anion polarizability ($Cl^- < Br^- < I^-$), while the intensity at around 3400 cm^{-1} increased with the same order. However, the dangling OH remained almost unchanged from that of the neat air/water interface, indicating an absence of these ions in the topmost water layer. The alkali cations are quite small and relatively nonpolarizable such that they have a much smaller effect on the water structure than the anion. Again, the spectral changes were interpreted as an interfacial enrichment of solvated polarizable anions (Br^-, I^-), which, on one hand, perturbs water hydrogen bonding beneath the topmost water layer and, on the other hand, creates a negative surface field that aligns more loosely bonded subphase water molecules. This was consistent with $\mathrm{Im}\,\chi_S^{(2)}$ spectra obtained on NaI solutions, which showed a more positive amplitude in the bonded OH below 3400 cm^{-1} indicative of the O−H stretching and field-induced reorientation of subsurface water molecules.[93,99] This also been confirmed by other surface-specific methods[52,130−133] and MD simulations.[41,42,134]

In comparison to halides, the surface affinity of large, polarizable molecular ions (e.g., ClO_4^-, CO_3^{2-}, NO_3^-, SO_4^{2-}, NH_4^+, etc.) have been much less studied experimentally. Nevertheless, several MD simulations have predicted a definite surface propensity of these ions at the air/water interface.[128,135−138] While halide anion surface affinity can be interpreted mostly in terms of their size and polarizability, these parameters appear to be insufficient when it comes to

dx.doi.org/10.1021/jz301179g | J. Phys. Chem. Lett. 2012, 3, 3012−3028

predicting partitioning of ions like CO_3^{2-}, NO_3^-, and SO_4^{2-}. Other factors such as surface charge density, ion geometry, solvation structure, and ion pairing can also play an important role in their surface affinity. For example, despite being singly charged and having comparable (isotropic) polarizability ($\alpha_0(Br^-) \approx 4.47$ Å^3 versus $\alpha_0(NO_3^-) \approx 4.6$ Å^3),[138,139] nitrate and bromide ions exhibit very different surface affinities. For monovalent nitrate salt solutions, conventional VSFG spectroscopy studies have shown a strong decrease in intensity in both 3200 and 3400 cm^{-1} regions;[63,123] however, the dangling OH region remains practically unchanged. These spectral changes have been attributed to the presence of NO_3^- ions at the interface. Recent PS-VSFG studies have observed a positive increase of Im $\chi^{(2)}$ for $NaNO_3$ solutions, thus indicating the presence of an EDL formed by NO_3^- ions with Na^+ co-ions repelled from the interface and the generation of a negative surface field reorienting water molecules toward the air.[63] It was shown that the surface propensity of NO_3^- ions lies somewhere between that of I^- and Na^+ ions, although as to whether it has a negative or positive surface excess still remains unclear. For instance, different MD simulations predicting the surface excess of NO_3^- ions at the air/water interface have suggested contradictory results.[135,137,138] Similarly, XPS measurements on concentrated $NaNO_3$ solutions revealed a depletion of NO_3^- ions from the interface,[140] while UV-SHG spectroscopy found instead a substantial surface excess.[141] In contrast to monovalent nitrate solutions, concentrated ($\gtrsim$3 M) divalent solutions ($Mg(NO_3)_2$, $Ca(NO_3)_2$, $Sr(NO_3)_2$) exhibited an enhancement in the 3400 cm^{-1} region whose intensity increases with increasing cation polarizability ($Mg^{2+} < Ca^{2+} < Sr^{2+}$) and concentration (Figure 4).[57] It was postulated that

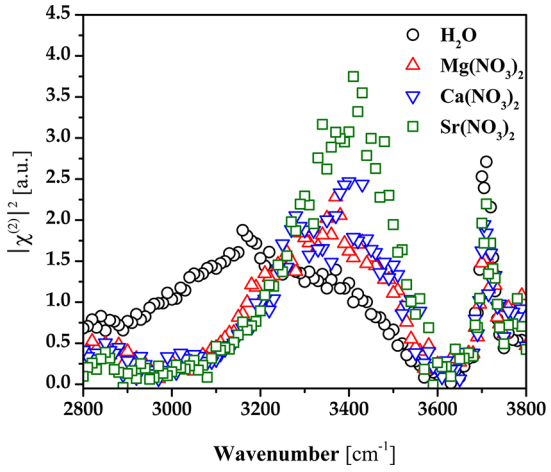

Figure 4. ssp-Polarized conventional VSFG spectra of nitrate salt solutions in the OH stretching region. All solutions had a concentration of 3.3 M (adapted from ref 57, copyright 2009, RSC Publishing).

cation−anion interactions affect the NO_3^- ion surface propensity and possibly create concentration gradients, thereby increasing the thickness of the interfacial region but not of the EDL because the intensity in the 3200 cm^{-1} region decreases. However, this interpretation still needs to be validated by further PS-VSFG studies.

Along with nitrates, sulfate salts are also of interest. SO_4^{2-} ions are doubly charged ions with a polarizability ($\alpha_0 \approx 7$ Å^3)[142] larger than that of most halides (except I^-). Nevertheless, SO_4^{2-} ions are repelled even farther away from the interface. In fact, conventional VSFG results on monovalent sulfate solutions (Na_2SO_4, $(NH_4)_2SO_4$) have shown a strong enhancement over the whole bonded OH stretching region, which extends to the lower-frequency region (Figure 5A).[63,64,126,136] Contrary to

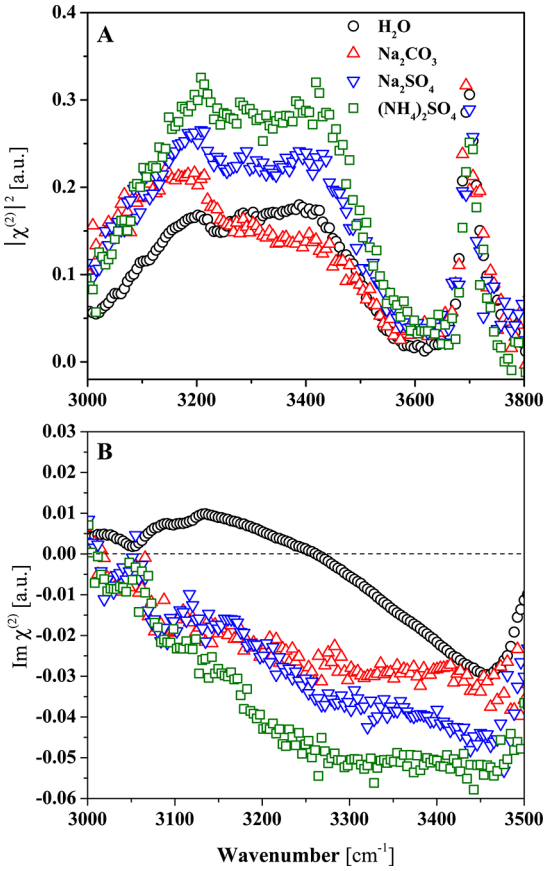

Figure 5. ssp-Polarized conventional VSFG (A) and PS-VSFG (B) spectra of salt solutions for selected molecular ions in the OH stretching region. All solutions had a concentration of 1.1 M (adapted from ref 64).

nitrate salts, the dissolution of sulfate salts results in the formation of a subsurface EDL with Na^+ ions now residing (on average) above SO_4^{2-} ions, thus creating a positive surface electric field whose effect on water alignment is evidenced by the enhancement in the 3200 cm^{-1} region. These findings are supported by recent PS-VSFG studies that show negative Im $\chi^{(2)}$ spectra for both Na_2SO_4 and $(NH_4)_2SO_4$ solutions, pointing at a net orientation of water OH transition dipole moments toward the bulk solution (Figure 5B).[63] Moreover, the greater magnitude of Im $\chi^{(2)}$ resolved for $(NH_4)_2SO_4$ solutions relative to Na_2SO_4 solutions has been attributed to the surface preference of the NH_4^+ ion. This molecular view is also consistent with MD simulations that predict greater propensity of the SO_4^{2-} ions for the bulk in comparison to Na^+ and NH_4^+.[136,142]

Another atmospherically relevant ion, CO_3^{2-}, has also received much attention lately. Despite being doubly charged like SO_4^{2-} ions, conventional VSFG studies on Na_2CO_3 solutions have shown that the presence of CO_3^{2-} causes rather a large intensity enhancement at and below 3200 cm^{-1} as well as a decrease at ~3400 cm^{-1} compared to the neat water interface (Figure 5A).[143] These results were interpreted as arising from a combination of hydrogen bonds strengthening

dx.doi.org/10.1021/jz301179g | J. Phys. Chem. Lett. 2012, 3, 3012−3028

and ion-induced water ordering. Other VSFG studies and MD simulations on Na_2CO_3 solutions later confirmed the increase in strong hydrogen bonding.[64,144,145] However, with the help of PS-VSFG spectroscopy, additional effects have since been identified. In comparison to the neat water interface, the Im $\chi^{(2)}$ spectrum show significant changes such as sign inversion in the 3000−3200 cm^{-1} region from positive to negative and an increased negative amplitude from 3200 to 3450 cm^{-1} (Figure 5B). The negative sign and strong amplitude of Im $\chi^{(2)}$ reveal a large fraction of interfacial water molecules with their O−H dipole moments oriented toward the bulk solution.[64,145] Like in the case SO_4^{2-} ions, these results could be explained by the presence of a positive surface electric field induced by an EDL with near-surface Na^+ ions and CO_3^{2-} ions residing at the bottom edge of the interfacial region.

Nonionic and Amphiphilic Solutes at Aqueous Solution Interfaces. Aside from inorganic ions, the adsorption of organic solutes has also a concrete effect on water organization at air/aqueous solution interfaces. For example, biogenic dimethylsulfide (DMS) produced by metabolic processes of marine phytoplankton plays an important role in atmospheric chemistry by being essential to the global sulfur cycle.[146,147] At the marine boundary layer, aqueous DMS is transferred to the gas phase and later photo-oxidized into sulfur-containing intermediates such as dimethylsulfoxide (DMSO, $(CH_3)_2S{=}O$), dimethyl sulfone (DMSO$_2$, $(CH_3)_2SO_2$), methanesulfonic acid (MSA, CH_3SO_2OH), and sulfuric acid (H_2SO_4).[148] Because of the strong water affinity of these organosulfur compounds, atmospheric sulfated aerosols that evolve from biogenically derived DMS emissions can then serve as cloud condensation nuclei, which, in turn, modify the global cloud cover, thus ultimately affecting Earth's albedo and climate.[149,150]

As such, the growth and, to some extent, the formation of aerosols initiated by DMSO and MSA relate to their interactions with water vapor, which addresses the importance of understanding interfacial water organization and its perturbation by these compounds. Previous studies made with conventional VSFG spectroscopy on aqueous DMSO and MSA solutions in the water hydrogen-bonding OH region (3000−3600 cm^{-1}) have shown that DMSO[151] induces only weak perturbations to the neat air/water interface, while MSA[152] produces a significant red shift that has been assigned to an enhancement in the hydrogen-bonding strength of interfacial water (Figure 6A,B). Recent work from our group has confirmed these previous measurements and has furthermore shown a concentration-dependent decrease in the water unbound (dangling) OH region (~3700 cm^{-1}) in the presence of DMSO, which can be attributed to the replacement or hydrogen bonding of the topmost water molecules by DMSO. This free OH decrease with increasing DMSO concentration is also supported by previous MD simulations.[153]

It was previously shown by conventional VSFG in the C−H and S=O regions that both DMSO and MSA exhibits definite surface orientation with their CH_3 groups preferentially oriented upward.[154] However, DMSO S=O group points inward, slightly away from the surface, while that of dissociated MSA is practically normal to the interface. This orientation of DMSO and the formation of hydrogen bonding between interfacial water molecules of the topmost layer and the S=O moiety should cause reorientation of water dipoles, an effect that is dependent on DMSO bulk concentration. This has been also predicted through MD simulations of DMSO−water

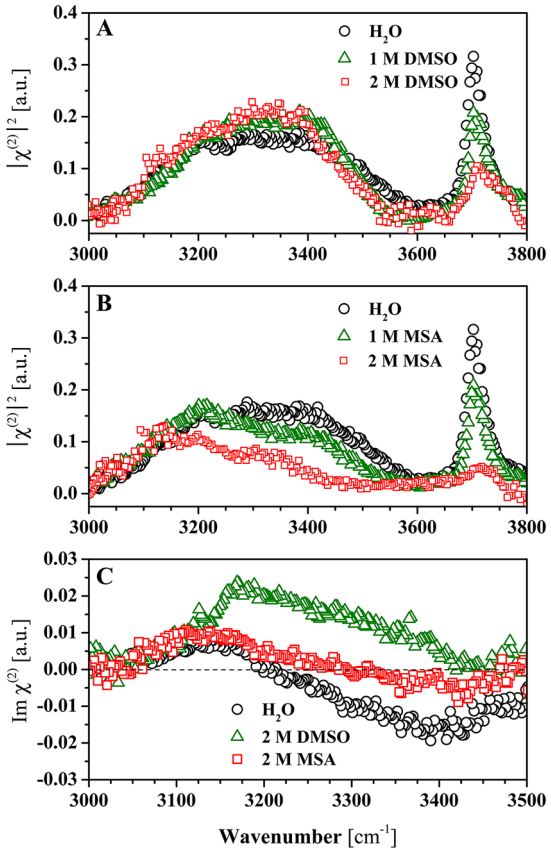

Figure 6. ssp-Conventional VSFG (A,B) and PS-VSFG (C) spectra in the hydrogen-bonded OH stretching region of neat water as well as DMSO and MSA aqueous solutions (adapted from ref 156).

mixtures.[155] However, conventional VSFG spectra show only small differences between 1 and 2 M aqueous DMSO solutions (Figure 6B). With the help of PS-VSFG, it was later shown by our group that for 2 M DMSO solution, the hydrogen-bonding network of interfacial water molecules is in fact greatly perturbed.[156] As shown in Figure 6C, the positive value of Im $\chi^{(2)}$ indicates that the presence of DMSO causes a reorientation of the interfacial water molecules with their dipole moment oriented on average toward the vapor phase. In contrast, the PS-VSFG spectrum of MSA reveals a lack of net water dipole moment orientation with a near-zero Im $\chi^{(2)}$ value in the bound OH region above 3200 cm^{-1}. This has been attributed to the competitive adsorption of both methanesulfonate anions and hydronium ions at and near the interfacial region.[127,152] The slightly higher surface propensity of methanesulfonate anions, as evidenced by their relative impact on the dangling OH region, creates a thin EDL in which the anion's charge is effectively screened by the hydronium ions, thereby inducing only minimal reorientation of water molecules. In this respect, PS-VSFG spectroscopy provided more insights into the water organization and orientation in the interfacial region in the presence of DMSO and MSA in comparison to conventional VSFG spectroscopy.

Lipid/aqueous interfaces are another important class of interfaces for which interfacial water organization play an important role. Examples of such interfaces are found with monolayer and bilayer systems such as Langmuir monolayers and micelles, and vesicles and bilayers, respectively. These systems usually serve as models of more realistic complex

dx.doi.org/10.1021/jz301179g | J. Phys. Chem. Lett. 2012, 3, 3012−3028

assemblies like biological membranes as well as organic-coated atmospheric marine aerosols. These assemblies usually consist of a lipid matrix, typically made of fatty acids, phospholipids, and sterols, in which various macromolecules like carbohydrates, nucleic acids, and proteins are embedded. Under environmental or physiological conditions, these lipid molecules are usually charged and surrounded by an aqueous phase containing various ionic species. Hence, the electrochemical behavior of these assemblies is strongly influenced by their environmental conditions such as ionic strength and pH.

Fatty acids and phospholipids are major constituents of the membrane structural backbone, whose unique ability to self-assembly arises from the amphiphilic nature of their structure and their interactions with the polar water environment. Amphiphilicity is conferred by two dissimilar regions, the hydrophobic tail group(s) made by alkyl chains of varying lengths and unsaturation and a hydrophilic head group, a negatively charged phosphate group linked to a diverse set of functional groups. The tail groups usually interact with each other in order to escape the surrounding water environment, while the head groups are immersed in the aqueous phase and are hydrated to varying degree. It is now well recognized that water molecules in the vicinity of the head group form strong hydrogen bonds with the phosphate and carbonyl moieties, with preference for the former group.[157] Concurrently, the electrostatic potential created by the charged head groups leads to ordering of the water dipoles and results in stronger hydrogen bonds between neighboring water molecules. The polarizing effect of phospholipid head groups is thus expected to be stronger for monolayers made up of negatively charged (anionic) lipids such as phosphatidic acid (PA), phosphatidylglycerol (PG), and phosphatidylserine (PS) compared to those consisting of zwitterionic lipids like phosphatidylcholine (PC) and phosphatidylethanolamine (PE). Despite their importance, a complete picture of water organization at simple lipid/aqueous interfaces has so far been only partly investigated.

Studies by conventional VSFG on phospholipids with different head groups (PC, PE, PG, PS) have shown that their adsorption translates into an absence of signal in the dangling OH region.[158,159] In addition, it was shown that the presence of the phospholipid monolayers caused a change in the distribution and the intensity of the bound OH region compared to that of the neat air/water interface, which was attributed to an increase in water molecule alignment perpendicular to the interface as well as an increase in probing depth. As expected, anionic phospholipids showed a larger signal enhancement in the bound OH region than zwitterionic ones because of the high electric potential generated by the negatively charged head group.[158,160] The enhancement was stronger in the 3200 cm^{-1} region for all phospholipids, which corresponds to high coordination between water molecules neighboring the phospholipids. More recent studies from our group with conventional VSFG spectroscopy found spectra that are consistent with other previously published work,[158] albeit with slightly lower intensities in the 3200 cm^{-1} region (Figure 7A).[161]

MD simulated VSFG spectra from the dimyristoylphosphatidylcholine (DMPC)/water interface have suggested that water dipoles are pointing upward and that the main contribution to the VSFG signal comes from the hydrophilic PC head group rather than the neighboring water molecules.[162] These results have hinted at the fact that the PC head group can be viewed as having a small net negative charge despite its

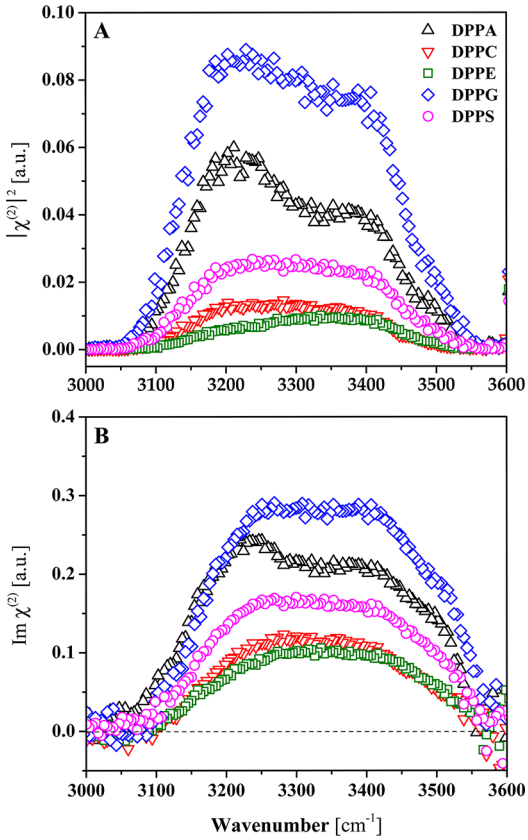

Figure 7. ssp-Polarized conventional VSFG (A) and PS-VSFG (B) spectra of anionic (DPPA, DPPG, DPPS) and zwitterionic (DPPC, DPPE) phospholipid monolayers in the hydrogen-bonded OH stretching region (adapted from ref 161).

zwitterionic character. This is in agreement with PS-VSFG measurements of anionic (PA, PG, PS) and zwitterionic (PC, PE) phospholipid monolayers that all exhibit positive Im $\chi^{(2)}$ values over the whole hydrogen-bonded OH stretching region compared to the neat water surface, with interfacial water molecules oriented on average toward the vapor phase (Figure 7B). Again, the lower intensity of dipalmitoylphosphatidylcholine (DPPC) and dipalmitoylphosphatidylethanolamine (DPPE) monolayers in comparison to that of anionic phospholipids suggests a weaker water polarizing effect. It was suggested that DPPC and DPPE mainly perturb water molecules between the tail carbonyl and head group choline groups, while the negatively charged head groups of anionic phospholipids (e.g., dipalmitoylphosphatidylglycerol (DPPG)) could influence water orientation over a longer range (Figure 8).[161] Due to their larger overall negative charge, the orientationally averaged total transition dipole moment (μ_{tot}) of water is greater in the presence of anionic phospholipids.

More recently, PS-VSFG results obtained on zwitterionic surfactant/water interface and on mixed anionic−cationic lipid/water interface lead to the conclusion that three distinct water structures should coexist at the zwitterionic lipid (PC)/water interface, each with different hydrogen-bonding interactions and orientation.[163] For instance, negative and positive bands of the Im $\chi^{(2)}$ spectra of the zwitterionic surfactant/water interface in the OH stretching region demonstrated the presence of two water species, one weakly hydrogen-bonded, oriented downward in the vicinity of the positively charged choline group, and another one strongly hydrogen-bonded, oppositely oriented in

dx.doi.org/10.1021/jz301179g | J. Phys. Chem. Lett. 2012, 3, 3012−3028

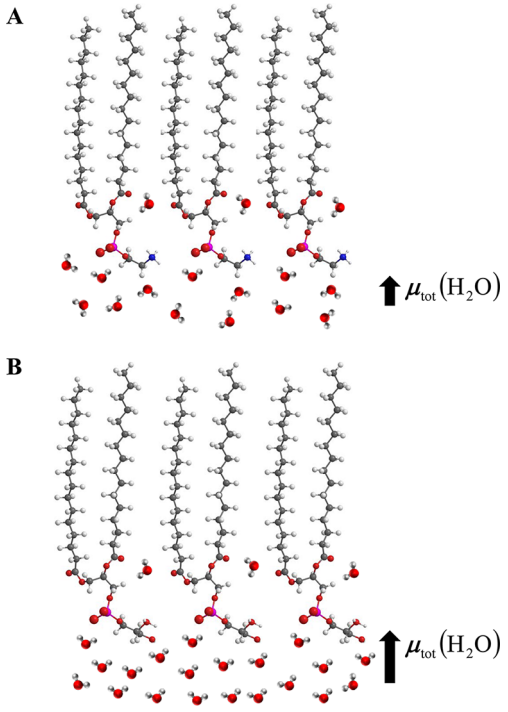

Figure 8. Schematic representation of water polarization at the zwitterionic (top) and anionic (bottom) lipid/water interfaces. (A) DPPE and (B) DPPG.

the vicinity of the negatively charged phosphate group. Finally, positive OH stretching bands at around 3600 cm^{-1} were also observed and interpreted as water weakly interacting with the hydrophobic portion of the lipid and in an upward orientation, thus providing valuable insight into the microenvironment of lipid head groups and solvation.

Summary and Future Directions. With the help of surface-specific nonlinear optical techniques such as conventional VSFG and PS-VSFG spectroscopies, further insight has been gained into understanding water molecular organization at aqueous interfaces and its perturbation arising from interactions with various ions and solutes. Application of both these techniques, often in combination with MD simulations and cluster models, has proven quite successful in unraveling the water orientation due to the presence of ions and other charged chemical groups. In particular, PS-VSFG spectroscopy has enabled discrimination of the influence of different charged chemical groups in more complex solutes (e.g., phospholipids).

Application of conventional VSFG and PS-VSFG spectroscopies, often in combination with MD simulations and cluster models, has proven quite successful in unraveling the water orientation due to the presence of ions and other charged chemical groups.

Despite substantial progress, obtaining a complete and detailed microscopic picture of water's hydrogen-bonding network at aqueous interfaces still remains a formidable challenge. For example, VSFG spectroscopic data obtained with inorganic ions at the air/water interface has shown that ion surface propensity cannot always be predicted based solely on just a few ion parameters (e.g., size, polarizability, or surface charge density). This is especially true when it comes to explaining so-called ion-specific effects occurring at aqueous "soft" (lipid monolayers, polymers, proteins) and solid (mineral oxides) interfaces.[164−168] Other parameters (hydration effects, ion correlations, ion geometry, etc.) also appear to play an important role in ion partitioning. Moreover, ion effects also depend strongly on the environment, more specifically on the counterions or chemical groups (e.g., lipid head groups, mineral surface groups) in their vicinity. Nevertheless, considerable efforts are currently being made to bridge the gap between experimental and computational views. The implementation of PS-VSFG spectroscopy marks a huge step toward this goal.

Although conventional broad-band VSFG spectroscopy and its adaptation for phase detection have so far been confined to only few research groups,[79,81,83,84,161] partly due to the prohibitive high costs of broad-band SFG systems and to the added instrumental complexity of the phase detection mode, it still remains among the best available surface-specific methods to study aqueous interfaces. To date, the combined conventional VSFG/PS-VSFG approach has been limited to a small number of aqueous interfaces, some of which have been presented in this work. Nevertheless, a substantial amount of work still remains to be done on these systems as well as on other important but perhaps less studied aqueous interfaces. Among possible research directions, some of which are currently pursued in our group, the influence of ion charge, geometry, and size as well as the type of countercations on the ion distribution at the air/water interface needs to be fully elucidated. Particularly, the cation−anion interactions in the case of chlorides, nitrates, and sulfate salts have not been systematically investigated. Also, the surface affinity of other relevant atmospheric aerosol species such as small organic acids and organic ions also deserves to be further studied.[169−173] Another topic concerns physiologically relevant cations and other ion-specific interactions with soft aqueous interfaces including, among others, phospholipid and fatty acid monolayers,[174,175] as well as their mixtures,[160] amphoteric brush-like polymers,[176−178] protein monolayers,[179] as well as hydrophilic/hydrophobic films[180] and self-assembled monolayers (SAMs).[181] Finally, water organization and ion-specific interactions at another important environment not covered in this Perspective, namely, mineral/aqueous interfaces, also need to be furthered. The interest for these interfaces and, in particular, those involving mineral oxides has increased significantly due to their environmental (e.g., aerosols and soils) and industrial relevance.[182−184] To date, conventional VSFG studies have mainly focused on investigating the effects of pH, ionic strength, and ion specificity on water hydrogen bonding at minerals of geological and/or industrial relevance such as fluorite (CaF_2)[185−187] and several oxides such as corundum (α-Al_2O_3),[188−190] quartz (α-SiO_2), fused silica,[191−197] and rutile (α-TiO_2).[196−198] In contrast, limited studies of these systems have so far been undertaken with PS-VSFG spectroscopy.[79,199]

Besides PS-VSFG spectroscopy, other complementary developments of VSFG spectroscopy have recently emerged and have already provided further insights into other aspects of aqueous interfaces. For example, ultrafast time-resolved (TR)-VSFG spectroscopy has been shown to be very useful in unraveling on a subpicosecond time scale water dynamics,

dx.doi.org/10.1021/jz301179g | J. Phys. Chem. Lett. 2012, 3, 3012−3028

including vibrational energy transfer, reorientational motion, and its perturbation by ions.[200,201] Particularly, it has been used to probe the O−H stretching vibrational lifetime and reorientation of interfacial water molecules at neat air/water,[202−204] lipid/water,[205,206] and mineral/water interfaces.[207−209] Another example comes from implementation of two-dimensional (2D)-VSFG spectroscopy, which provides direct information about interfacial inhomogeneity, vibrational mode couplings, and chemical exchange.[210,211] This novel technique has enabled, for instance, the measurement of intra- and intermolecular vibrational energy transfer between hydrogen-bonded and straddling interfacial water molecules.[212,213] Finally, the advent of an ultrabroad-band IR source based on the noncollinear optical parametric amplifier technology allows conventional broad-band SFG spectrometers to acquire the entire water spectrum over a frequency range comparable to scanning SFG systems but without IR tuning and on a much shorter (seconds) time scale.[214] Clearly, all of these advances will have a positive effect for understanding aqueous interfaces.

AUTHOR INFORMATION

Corresponding Author

*E-mail: allen@chemistry.ohio-state.edu.

Notes

The authors declare no competing financial interest.

Biographies

Dominique Verreault obtained his Ph.D. in Physical Chemistry in 2011 from the University of Heidelberg, Heidelberg (Germany), under the direction of Prof. Michael Grunze. He is currently a postdoctoral researcher in the Department of Chemistry and Biochemistry at The Ohio State University, where he is applying vibrational spectroscopic methods in the study of ion interactions and ion-specific effects at the air/water and mineral/water interfaces.

Wei Hua obtained her B.S. in Chemistry in 2005 and M.S. in Environmental Sciences in 2008 from Peking University, Peking (China), under the direction of Prof. Zhongming Chen. Since 2008, she has been pursuing her Ph.D. degree in the Department of Chemistry and Biochemistry at The Ohio State University, under the direction of Prof. Heather C. Allen. Her research interests are focused on aqueous surface structure and molecular interactions in atmospheric chemistry and biologically relevant monolayer systems.

Heather C. Allen received her Ph.D. in Physical Chemistry in 1997 from the University of California, Irvine, under the direction of Professors John C. Hemminger and Barbara J. Finlayson-Pitts. She is currently professor in the Department of Chemistry and Biochemistry as well as in the Department of Pathology at The Ohio State University. Her research focuses on studying interfacial systems of biological and environmental relevance such as cell membranes, atmospheric aerosols, cancerous tissues, cloud microdroplets, and mineral surfaces using vibrational spectroscopic and imaging techniques. http://research.chemistry.ohio-state.edu/allen.

ACKNOWLEDGMENTS

The authors gratefully acknowledge the NSF-CHE (Grants 0749807 and 1111762) and the DOE-BES Geochemistry (Grant DE-FG02-04ER15495) for funding this work. The authors would also like to thank Dr. C. Tang for providing a figure for the Table of Contents and Dr. I. Stiopkin, formerly from the Benderskii group, for his helpful suggestions in the development of our PS-VSFG setup.

REFERENCES

(1) Ball, P. *H_2O: A Biography of Water*; Weidenfeld & Nicolson: London, 1999.

(2) Finney, J. L. Water? What's so Special About it? *Philos. Trans. R. Soc. London, Ser. B* **2004**, *359*, 1145−1165.

(3) Ball, P. Water as an Active Constituent in Cell Biology. *Chem. Rev.* **2008**, *108*, 74−108.

(4) Brovchenko, I.; Oleinikova, A. *Interfacial and Confined Water*; Elsevier Science: New York, 2008.

(5) Fayer, M. D.; Levinger, N. E. Analysis of Water in Confined Geometries and at Interfaces. *Annu. Rev. Anal. Chem.* **2010**, *3*, 89−107.

(6) Fayer, M. D. Dynamics of Water Interacting with Interfaces, Molecules, and Ions. *Acc. Chem. Res.* **2012**, *45*, 3−14.

(7) Lang, E. W.; Ludemann, H. D. The Anomalous Properties of Liquid Water. *Angew. Chem., Int. Ed.* **1982**, *21*, 315−388.

(8) Brovchenko, I.; Oleinikova, A. Multiple Phases of Liquid Water. *ChemPhysChem* **2008**, *9*, 2660−2675.

(9) Cheng, L.; Fenter, P.; Nagy, K. L.; Schlegel, M. L.; Sturchio, N. C. Molecular-Scale Density Oscillations in Water Adjacent to a Mica Surface. *Phys. Rev. Lett.* **2001**, *87*, 156103/1−156103/4.

(10) Teschke, O.; Ceotto, G.; de Souza, G. F. Interfacial Water Dielectric-Permittivity-Profile Measurements using Atomic Force Microscopy. *Phys. Rev. E* **2001**, *64*, 011605/1−011605/10.

(11) Bonthuis, D. J.; Gekle, S.; Netz, R. R. Profile of the Static Permittivity Tensor of Water at Interfaces: Consequences for Capacitance, Hydration Interaction and Ion Adsorption. *Langmuir* **2012**, *28*, 7679−7694.

(12) Goertz, M. P.; Houston, J. E.; Zhu, X. Y. Hydrophilicity and the Viscosity of Interfacial Water. *Langmuir* **2007**, *23*, 5491−5497.

(13) Vargaftik, N. B.; Volkov, B. N.; Voljak, L. D. International Tables of the Surface Tension of Water. *J. Phys. Chem. Ref. Data* **1983**, *12*, 817−820.

(14) Sokhan, V. P.; Tildesley, D. J. The Free Surface of Water: Molecular Orientation, Surface Potential and Nonlinear Susceptibility. *Mol. Phys.* **1997**, *92*, 625−640.

(15) Paluch, M. Electrical Properties of Free Surface of Water and Aqueous Solutions. *Adv. Colloid Interface Sci.* **2000**, *84*, 27−45.

(16) Parfenyuk, V. I. Surface Potential at the Gas−Aqueous Solution Interface. *Colloid J.* **2002**, *64*, 588−595.

(17) Kathmann, S. M.; Kuo, I.-F. W.; Mundy, C. J.; Schenter, G. K. Understanding the Surface Potential of Water. *J. Phys. Chem. B* **2011**, *115*, 4369−4377.

(18) Vácha, R.; Marsalek, O.; Willard, A. P.; Bonthuis, D. J.; Netz, R. R.; Jungwirth, P. Charge Transfer between Water Molecules as the Possible Origin of the Observed Charging at the Surface of Pure Water. *J. Phys. Chem. Lett.* **2012**, *3*, 107−111.

(19) Vácha, R.; Buch, V.; Milet, A.; Devlin, J. P.; Jungwirth, P. Autoionization at the Surface of Neat Water: Is the Top Layer pH Neutral, Basic, or Acidic? *Phys. Chem. Chem. Phys.* **2007**, *9*, 4736−4747.

(20) Gray-Weale, A.; Beattie, J. K. An Explanation for the Charge on Water's Surface. *Phys. Chem. Chem. Phys.* **2009**, *11*, 10994−11005.

(21) Zimmermann, R.; Freudenberg, U.; Schweiß, R.; Küttner, D.; Werner, C. Hydroxide and Hydronium Ion Adsorption — A Survey. *Curr. Opin. Colloid Interface Sci.* **2010**, *15*, 196−202.

(22) Petersen, P. B.; Saykally, R. J. Is the Liquid Water Surface Basic or Acidic? Macroscopic vs. Molecular-Scale Investigations. *Chem. Phys. Lett.* **2008**, *458*, 255−261.

(23) Jungwirth, P.; Winter, B. Ions at Aqueous Interfaces: From Water Surface to Hydrated Proteins. *Annu. Rev. Phys. Chem.* **2008**, *59*, 343−366.

(24) Jubb, A. M.; Hua, W.; Allen, H. C. Organization of Water and Atmospherically Relevant Ions and Solutes: Vibrational Sum Frequency Spectroscopy at the Vapor/Liquid and Liquid/Solid Interfaces. *Acc. Chem. Res.* **2012**, *45*, 110−119.

(25) Jubb, A. M.; Hua, W.; Allen, H. C. Environmental Chemistry at Vapor/Water Interfaces: Insights from Vibrational Sum Frequency Generation Spectroscopy. *Annu. Rev. Phys. Chem.* **2012**, *63*, 107−130.

(26) Netz, R. R.; Horinek, D. Progress in Modeling of Ion Effects at the Vapor/Water Interface. *Annu. Rev. Anal. Chem.* **2012**, *63*, 401−418.
(27) Onsager, L.; Samaras, N. N. T. The Surface Tension of Debye−Hückel Electrolytes. *J. Chem. Phys.* **1934**, *2*, 528−536.
(28) Chang, T. M.; Dang, L. X. Recent Advances in Molecular Simulations of Ion Solvation at Liquid Interfaces. *Chem. Rev.* **2006**, *106*, 1305−1322.
(29) Jungwirth, P.; Tobias, D. J. Specific Ion Effects at the Air/Water Interface. *Chem. Rev.* **2006**, *106*, 1259−1281.
(30) Gopalakrishnan, S.; Liu, D. F.; Allen, H. C.; Kuo, M.; Shultz, M. J. Vibrational Spectroscopic Studies of Aqueous Interfaces: Salts, Acids, Bases, and Nanodrops. *Chem. Rev.* **2006**, *106*, 1155−1175.
(31) Winter, B.; Faubel, M. Photoemission from Liquid Aqueous Solutions. *Chem. Rev.* **2006**, *106*, 1176−1211.
(32) Marcus, Y. Effect of Ions on the Structure of Water: Structure Making and Breaking. *Chem. Rev.* **2009**, *109*, 1346−1370.
(33) Collins, K. D.; Neilson, G. W.; Enderby, J. E. Ions in Water: Characterizing the Forces that Control Chemical Processes and Biological Structure. *Biophys. Chem.* **2007**, *128*, 95−104.
(34) Stuart, S. J.; Berne, B. J. Surface Curvature Effects in the Aqueous Ionic Solvation of the Chloride Ion. *J. Phys. Chem. A* **1999**, *103*, 10300−10307.
(35) Noah-Vanhoucke, J.; Geissler, P. L. Liquids and Structural Glasses Special Feature: On the Fluctuations that Drive Small Ions Toward, and Away from, Interfaces between Polar Liquids and Their Vapors. *Proc. Natl. Acad. Sci. U.S.A.* **2009**, *106*, 15125−15130.
(36) Otten, D. E.; Shaffer, P. R.; Geissler, P. L.; Saykally, R. J. Elucidating the Mechanism of Selective Ion Adsorption to the Liquid Water Surface. *Proc. Natl. Acad. Sci. U.S.A.* **2012**, *109*, 701−705.
(37) Peslherbe, G. H.; Ladanyi, B. M.; Hynes, J. T. Structure of NaI Ion Pairs in Water Clusters. *Chem. Phys.* **2000**, *258*, 201−224.
(38) Herce, D. H.; Perera, L.; Darden, T. A.; Sagui, C. Surface Solvation for an Ion in a Water Cluster. *J. Chem. Phys.* **2005**, *122*, 024513/1−024513/10.
(39) Archontis, G.; Leontidis, E.; Andreou, G. Attraction of Iodide Ions by the Free Water Surface, Revealed by Simulations with a Polarizable Force Field Based on Drude Oscillators. *J. Phys. Chem.* **2005**, *109*, 17957−17966.
(40) Wick, C. D.; Xantheas, S. S. Computational Investigation of the First Solvation Shell Structure of Interfacial and Bulk Aqueous Chloride and Iodide Ions. *J. Phys. Chem. B* **2009**, *113*, 4141−4146.
(41) Jungwirth, P.; Tobias, D. J. Molecular Structure of Salt Solutions: A New View of the Interface with Implications for Heterogeneous Atmospheric Chemistry. *J. Phys. Chem. B* **2001**, *105*, 10468−10472.
(42) Jungwirth, P.; Tobias, D. J. Ions at the Air/Water Interface. *J. Phys. Chem. B* **2002**, *106*, 6361−6373.
(43) Pegram, L. M.; Record, M. T. Partitioning of Atmospherically Relevant Ions Between Bulk Water and the Water/Vapor Interface. *Proc. Natl. Acad. Sci. U.S.A.* **2006**, *103*, 14278−14281.
(44) Arslanargin, A.; Beck, T. L. Free Energy Partitioning Analysis of the Driving Forces that Determine Ion Density Profiles Near the Water Liquid−Vapor Interface. *J. Chem. Phys.* **2012**, *136*, 104503/1−104503/12.
(45) Baer, M. D.; Stern, A. C.; Levin, Y.; Tobias, D. J.; Mundy, C. J. Electrochemical Surface Potential Due to Classical Point Charge Models Drives Anion Adsorption to the Air−Water Interface. *J. Phys. Chem. Lett.* **2012**, *3*, 1565−1570.
(46) Cheng, J.; Vecitis, C. D.; Hoffmann, M. R.; Colussi, A. J. Experimental Anion Affinities for the Air/Water Interface. *J. Phys. Chem. B* **2006**, *110*, 25598−25602.
(47) Wren, S. N.; Donaldson, D. J. Glancing-Angle Raman Spectroscopic Probe for Reaction Kinetics at Water Surfaces. *Phys. Chem. Chem. Phys.* **2010**, *12*, 2648−2654.
(48) Wren, S. N.; Donaldson, D. J. Exclusion of Nitrate to the Air−Ice Interface During Freezing. *J. Phys. Chem. Lett.* **2011**, *2*, 1967−1971.
(49) Miller, D. J.; Lisy, J. M. Hydrated Alkali-Metal Cations: Infrared Spectroscopy and ab Initio Calculations of $M^+(H_2O)_{x=2-5}Ar$ Cluster Ions for M = Li, Na, K, and Cs. *J. Am. Chem. Soc.* **2008**, *130*, 15381−15392.
(50) Asmis, K. R.; Neumark, D. M. Vibrational Spectroscopy of Microhydrated Conjugate Base Anions. *Acc. Chem. Res.* **2012**, *45*, 43−52.
(51) Padmanabhan, V.; Daillant, J.; Belloni, L.; Mora, S.; Alba, M.; Konovalov, O. Specific Ion Adsorption and Short-Range Interactions at the Air Aqueous Solution Interface. *Phys. Rev. Lett.* **2007**, *99*, 086105/1−086105/4.
(52) Ghosal, S.; Hemminger, J. C.; Bluhm, H.; Mun, S. M.; Hebenstreit, E. L. D.; Ketteler, G.; Ogletree, D. F.; Requejo, F. G.; Salmeron, M. Electron Spectroscopy of Aqueous Solution Interfaces Reveals Surface Enhancement of Halides. *Science* **2005**, *307*, 563−566.
(53) Eisenthal, K. B. Liquid Interfaces Probed by Second-Harmonic and Sum-Frequency Spectroscopy. *Chem. Rev.* **1996**, *96*, 1343−1360.
(54) Eisenthal, K. B. Second Harmonic Spectroscopy of Aqueous Nano- and Microparticle Interfaces. *Chem. Rev.* **2006**, *106*, 1462−1477.
(55) Petersen, P. B.; Saykally, R. J. On the Nature of Ions at the Liquid Water Surface. *Annu. Rev. Phys. Chem.* **2006**, *57*, 333−364.
(56) Schrödle, S.; Richmond, G. L. *In Situ* Non-Linear Spectroscopic Approaches to Understanding Adsorption at Mineral−Water Interfaces. *J. Phys. D: Appl. Phys.* **2008**, *41*, 033001/1−033001/14.
(57) Allen, H. C.; Casillas-Ituarte, N. N.; Sierra-Hernandez, M. R.; Chen, X. K.; Tang, C. Y. Shedding Light on Water Structure at Air−Aqueous Interfaces: Ions, Lipids, and Hydration. *Phys. Chem. Chem. Phys.* **2009**, *11*, 5538−5549.
(58) Petersen, P. B.; Johnson, J. C.; Knutsen, K. P.; Saykally, R. J. Confirmation of Enhanced Anion Concentration at the Liquid Water Surface. *Chem. Phys. Lett.* **2004**, *397*, 51−55.
(59) Onorato, R. M.; Otten, D. E.; Saykally, R. J. Measurement of Bromide Ion Affinities for the Air/Water and Dodecanol/Water Interfaces at Molar Concentrations by UV Second Harmonic Generation Spectroscopy. *J. Phys. Chem. C* **2010**, *114*, 13746−13751.
(60) Viswanath, P.; Motschmann, H. Oriented Thiocyanate Anions at the Air−Electrolyte Interface and Its Implications on Interfacial Water — A Vibrational Sum Frequency Spectroscopy Study. *J. Phys. Chem. C* **2007**, *111*, 4484−4486.
(61) Viswanath, P.; Motschmann, H. Effect of Interfacial Presence of Oriented Thiocyanate on Water Structure. *J. Phys. Chem. C* **2008**, *112*, 2099−2103.
(62) Xu, M; Tang, C. Y.; Jubb, A. M.; Chen, X. K.; Allen, H. C. Nitrate Anions and Ion Pairing at the Air−Aqueous Interface. *J. Phys. Chem. C* **2009**, *113*, 2082−2087.
(63) Tian, C.; Byrnes, S. J.; Han, H.-L.; Shen, Y. R. Surface Propensities of Atmospherically Relevant Ions in Salt Solutions Revealed by Phase-Sensitive Sum Frequency Vibrational Spectroscopy. *J. Phys. Chem. Lett.* **2011**, *2*, 1946−1949.
(64) Hua, W.; Jubb, A. M.; Allen, H. C. Electric Field Reversal of Na_2SO_4, $(NH_4)_2SO_4$, and Na_2CO_3 Relative to $CaCl_2$ and NaCl at the Air/Aqueous Interface Revealed by Heterodyne Detected Phase-Sensitive Sum Frequency. *J. Phys. Chem. Lett.* **2011**, *2*, 2515−2520.
(65) Heinz, T. F. Second-Order Nonlinear Optical Effects at Surfaces and Interfaces. In *Nonlinear Surface Electromagnetic Phenomena*; Ponath, H.-E., Stegemen, G. I., Eds.; North-Holland: Amsterdam, The Netherlands, 1991.
(66) Shen, Y. R. Surface Spectroscopy by Nonlinear Optics. In *Frontiers in Laser Spectroscopy: Proceedings of the International School of Physics "Enrico Fermi"*, Course CXX; Hänsch, T. W., Ignuscio, M., Eds.; North-Holland: Amsterdam, The Netherlands, 1994.
(67) Hunt, J. H.; Guyot-Sionnest, P.; Shen, Y. R. Observation of C−H Stretch Vibrations of Monolayers of Molecules Optical Sum-Frequency Generation. *Chem. Phys. Lett.* **1987**, *133*, 189−192.
(68) Zhu, X. D.; Suhr, H.; Shen, Y. R. Surface Vibrational Spectroscopy by Infrared−Visible Sum Frequency Generation. *Phys. Rev. B* **1987**, *35*, 3047−3050.
(69) Guyot-Sionnest, P.; Hunt, J. H.; Shen, Y. R. Sum-Frequency Vibrational Spectroscopy of a Langmuir Film: Study of Molecular

Orientation of a Two-Dimensional System. *Phys. Rev. Lett.* **1987**, *59*, 1597−1600.
(70) Zhuang, X.; Miranda, P. B.; Kim, D.; Shen, Y. R. Mapping Molecular Orientation and Conformation at Interfaces by Surface Nonlinear Optics. *Phys. Rev. B* **1999**, *59*, 12632−12640.
(71) Bain, C. D.; Davies, P. B.; Ong, T. H.; Ward, R. N.; Brown, M. A. Quantitative Analysis of Monolayer Composition by Sum-Frequency Vibrational Spectroscopy. *Langmuir* **1991**, *7*, 1563−1566.
(72) Feng, R.-r.; Guo, Y.; Lü, R.; Velarde, L.; Wang, H.-f. Consistency in the Sum Frequency Generation Intensity and Phase Vibrational Spectra of the Air/Neat Water Interface. *J. Phys. Chem. A* **2011**, *115*, 6015−6027.
(73) Busson, B.; Tadjeddine, A. Non-Uniqueness of Parameters Extracted from Resonant Second-Order Nonlinear Optical Spectroscopies. *J. Phys. Chem. C* **2009**, *113*, 21895−21902.
(74) Sovago, M.; Vartiainen, E.; Bonn, M. Determining Absolute Molecular Orientation at Interfaces: A Phase Retrieval Approach for Sum Frequency Generation Spectroscopy. *J. Phys. Chem. C* **2009**, *113*, 6100−6106.
(75) (a) Sovago, M.; Vartiainen, E.; Bonn, M. Observation of Buried Water Molecules in Phospholipid Membranes by Surface Sum-Frequency Generation Spectroscopy. *J. Chem. Phys.* **2009**, *131*, 161107/1−161107/4. (b) Sovago, M.; Vartiainen, E.; Bonn, M. Erratum: Observation of Buried Water Molecules in Phospholipid Membranes by Surface Sum-Frequency Generation Spectroscopy. *J. Chem. Phys.* **2010**, *133*, 229901/1−229901/2.
(76) de Beer, A. G. F.; Samson, J.-S.; Hua, W.; Huang, Z.; Chen, X.; Allen, H. C.; Roke, S. Direct Comparison of Phase-Sensitive Vibrational Sum Frequency Generation with Maximum Entropy Method: Case Study of Water. *J. Chem. Phys.* **2011**, *135*, 224701/1−224701/9.
(77) Superfine, R.; Huang, J. Y.; Shen, Y. R. Phase Measurement for Surface Infrared−Visible Sum-Frequency Generation. *Opt. Lett.* **1990**, *15*, 1276−1278.
(78) Superfine, R.; Huang, J. Y.; Shen, Y. R. Experimental Determination of the Sign of Molecular Dipole Moment Derivatives: An Infrared−Visible Sum Frequency Generation Absolute Phase Measurement Study. *Chem. Phys. Lett.* **1990**, *172*, 303−306.
(79) Ostroverkhov, V.; Waychunas, G. A.; Shen, Y. R. New Information on Water Interfacial Structure Revealed by Phase-Sensitive Surface Spectroscopy. *Phys. Rev. Lett.* **2005**, *94*, 046102/1−046102/4.
(80) Ji, N.; Ostroverkhov, V.; Chen, C.-Y.; Shen, Y.-R. Phase-Sensitive Sum-Frequency Vibrational Spectroscopy and Its Application to Studies of Interfacial Alkyl Chains. *J. Am. Chem. Soc.* **2007**, *129*, 10056−10057.
(81) Stiopkin, I. V.; Jayathilake, H. D.; Bordenyuk, A. N.; Benderskii, A. V. Heterodyne-Detected Vibrational Sum Frequency Generation Spectroscopy. *J. Am. Chem. Soc.* **2008**, *130*, 2271−2275.
(82) Yamaguchi, S.; Tahara, T. Heterodyne-Detected Electronic Sum Frequency Generation: "Up" versus "Down" Alignment of Interfacial Molecules. *J. Chem. Phys.* **2008**, *129*, 101102/1−101102/4.
(83) Nihonyanagi, S.; Yamaguchi, S.; Tahara, T. Direct Evidence for Orientational Flip-Flop of Water Molecules at Charged Interfaces: A Heterodyne-Detected Vibrational Sum Frequency Generation Study. *J. Chem. Phys.* **2009**, *130*, 204704/1−204704/5.
(84) Pool, R. E.; Versluis, J.; Backus, E. H. G.; Bonn, M. Comparative Study of Direct and Phase-Specific Vibrational Sum-Frequency Generation Spectroscopy: Advantages and Limitations. *J. Phys. Chem. B* **2011**, *115*, 15362−15369.
(85) Bloembergen, N.; Pershan, P. S. Light Waves at the Boundary of Nonlinear Media. *Phys. Rev.* **1962**, *128*, 606−622.
(86) Lü, R.; Rao, Y.; Zhang, W.-k.; Wang, H.-f. Phase Measurement in Nonlinear Optics of Molecules at Air/Water Interface with Femtosecond Laser Pulses. *Proc. SPIE Nonlinear Spectrosc.* **2002**, *4812−15*, 115−124.
(87) Jungwirth, P.; Finlayson-Pitts, B. J.; Tobias, D. J. Introduction: Structure and Chemistry at Aqueous Interfaces. *Chem. Rev.* **2006**, *106*, 1137−1139.
(88) Shultz, M. J.; Baldelli, S.; Schnitzer, C.; Simonelli, D. Aqueous Solution/Air Interfaces Probed with Sum Frequency Generation Spectroscopy. *J. Phys. Chem. B* **2002**, *106*, 5313−5324.
(89) Shen, Y. R.; Ostroverkhov, V. Sum-Frequency Vibrational Spectroscopy on Water Interfaces: Polar Orientation of Water Molecules at Interfaces. *Chem. Rev.* **2006**, *106*, 1140−1154.
(90) Morita, A.; Ishiyama, T. Recent Progress in Theoretical Analysis of Vibrational Sum Frequency Generation Spectroscopy. *Phys. Chem. Chem. Phys.* **2008**, *10*, 5801−5816.
(91) Skinner, J. L.; Pieniazek, P. A.; Gruenbaum, S. M. Vibrational Spectroscopy of Water at Interfaces. *Acc. Chem. Res.* **2012**, *45*, 93−100.
(92) Du, Q.; Superfine, R.; Freysz, E.; Shen, Y. R. Vibrational Spectroscopy of Water at the Vapor/Water Interface. *Phys. Rev. Lett.* **1993**, *70*, 2313−2316.
(93) Ji, N.; Ostroverkhov, V.; Tian, C. S.; Shen, Y. R. Characterization of Vibrational Resonances of Water−Vapor Interfaces by Phase-Sensitive Sum-Frequency Spectroscopy. *Phys. Rev. Lett.* **2008**, *100*, 096102/1−096102/4.
(94) Sovago, M.; Kramer Campen, R.; Wurpel, G. W. H.; Müller, M.; Bakker, H. J.; Bonn, M. Vibrational Response of Hydrogen-Bonded Interfacial Water is Dominated by Intramolecular Coupling. *Phys. Rev. Lett.* **2008**, *100*, 173901/1−173901/4.
(95) Sovago, M.; Kramer Campen, R.; Wurpel, G. W. H.; Müller, M.; Bakker, H. J.; Bonn, M. Sovago *et al.* Reply. *Phys. Rev. Lett.* **2008**, *101*, 139402/1.
(96) Tian, C. S.; Shen, Y. R. Sum-Frequency Vibrational Spectroscopic Studies of Water/Vapor Interfaces. *Chem. Phys. Lett.* **2009**, *470*, 1−6.
(97) Pieniazek, P. A.; Tainter, C. J.; Skinner, J. L. Interpretation of the Water Surface Vibrational Sum-Frequency Spectrum. *J. Chem. Phys.* **2011**, *135*, 044701/1−044701/12.
(98) Nihonyanagi, S.; Ishiyama, T.; Lee, T.-k.; Yamaguchi, S.; Bonn, M.; Morita, A.; Tahara, T. Unified Molecular View of the Air/Water Interface Based on Experimental and Theoretical $\chi^{(2)}$ Spectra of an Isotopically Diluted Water Surface. *J. Am. Chem. Soc.* **2011**, *133*, 16875−16880.
(99) Tian, C.; Ji, N.; Waychunas, G. A.; Shen, Y. R. Interfacial Structures of Acidic and Basic Aqueous Solutions. *J. Am. Chem. Soc.* **2008**, *130*, 13033−13039.
(100) Tian, C.-S.; Shen, Y. R. Isotopic Dilution Study of the Water/Vapor Interface by Phase-Sensitive Sum-Frequency Vibrational Spectroscopy. *J. Am. Chem. Soc.* **2009**, *131*, 2790−2791.
(101) Morita, A.; Hynes, J. T. A Theoretical Analysis of the Sum Frequency Generation Spectrum of the Water Surface. *Chem. Phys.* **2000**, *258*, 371−390.
(102) Morita, A.; Hynes, J. T. A Theoretical Analysis of the Sum Frequency Generation Spectrum of the Water Surface. II. Time-Dependent Approach. *J. Phys. Chem. B* **2002**, *106*, 673−685.
(103) Perry, A.; Ahlborn, H.; Space, B.; Moore, P. B. A Combined Time Correlation Function and Instantaneous Normal Mode Study of the Sum Frequency Generation Spectroscopy of the Water/Vapor Interface. *J. Chem. Phys.* **2003**, *118*, 8411/1−144705/9.
(104) Buch, V. Molecular Structure and OH-Stretch Spectra of Liquid Water Surface. *J. Phys. Chem. B* **2005**, *109*, 17771−17774.
(105) Perry, A.; Neipert, C.; Ridley Kasprzyk, C.; Green, T.; Space, B.; Moore, P. B. A Theoretical Description of the Polarization Dependence of the Sum Frequency Generation Spectroscopy of the Water/Vapor Interface. *J. Chem. Phys.* **2005**, *123*, 144705/1−144705/11.
(106) Morita, A. Improved Computation of Sum Frequency Generation Spectrum of the Surface of Water. *J. Phys. Chem. B* **2006**, *110*, 3158−3163.
(107) Perry, A.; Neipert, C.; Space, B.; Moore, P. B. Theoretical Modeling of Interface Specific Vibrational Spectroscopy: Methods and Applications to Aqueous Interfaces. *Chem. Rev.* **2006**, *106*, 1234−1258.
(108) Buch, V.; Tarbuck, T.; Richmond, G. L.; Groenzin, H.; Li, I.; Shultz, M. J. Sum Frequency Generation Surface Spectra of Ice, Water, and Acid Solution Investigated by an Exciton Model. *J. Chem. Phys.* **2007**, *127*, 204710/1−204710/15.

(109) Auer, B. M.; Skinner, J. L. Vibrational Sum-Frequency Spectroscopy of the Liquid/Vapor Interface for Dilute HOD in D_2O. *J. Chem. Phys.* **2008**, *129*, 214705/1−214705/14.
(110) Auer, B. M.; Skinner, J. L. Vibrational Sum-Frequency Spectroscopy of the Water Liquid/Vapor Interface. *J. Phys. Chem. B* **2009**, *113*, 4125−4130.
(111) Fan, Y.; Chen, X.; Yang, L.; Cremer, P. S.; Gao, Y. Q. On the Structure of Water at the Aqueous/Air Interface. *J. Phys. Chem. B* **2009**, *113*, 11672−11679.
(112) Ishiyama, T.; Morita, A. Vibrational Spectroscopic Response of Intermolecular Orientational Correlation at the Water Surface. *J. Phys. Chem. C* **2009**, *113*, 16299−16302.
(113) Pieniazek, P. A.; Tainter, C. J.; Skinner, J. L. Surface of Liquid Water: Three-Body Interactions and Vibrational Sum-Frequency Spectroscopy. *J. Am. Chem. Soc.* **2011**, *133*, 10360−10363.
(114) Finlayson-Pitts, B. J.; Pitts, J. N., Jr. *Chemistry of the Upper and Lower Atmosphere: Theory, Experiments, and Applications*; Academic Press: San Diego, CA, 2000.
(115) Finlayson-Pitts, B. Reactions at Surfaces in the Atmosphere: Integration of Experiments and Theory as Necessary (but not Necessarily Sufficient) for Predicting the Physical Chemistry of Aerosols. *Phys. Chem. Chem. Phys.* **2009**, *11*, 7760−7779.
(116) Foster, K. L.; Plastridge, R. A.; Bottenheim, J. W.; Shepson, P. B.; Finlayson-Pitts, B. J.; Spicer, C. W. The Role of Br_2 and BrCl in Surface Ozone Destruction at Polar Sunrise. *Science* **2001**, *291*, 471−474.
(117) Spicer, C. W.; Plastridge, R. A.; Foster, K. L.; Finlayson-Pitts, B. J.; Bottenheim, J. W.; Grannas, A. M.; Shepson, P. B. Molecular Halogens Before and During Ozone Depletion Events in the Arctic at Polar Sunrise: Concentrations and Sources. *Atmos. Environ.* **2002**, *36*, 2721−2731.
(118) Finlayson-Pitts, B. J. Halogens in the Troposphere. *Anal. Chem.* **2010**, *82*, 770−776.
(119) Hunt, S. W.; Roeselova, M.; Wang, W.; Wingen, L. M.; Knipping, E. M.; Tobias, D. J.; Dabdub, D.; Finlayson-Pitts, B. J. Formation of Molecular Bromine from the Reaction of Ozone with Deliquesced NaBr Aerosol: Evidence for Interface Chemistry. *J. Phys. Chem. A* **2004**, *108*, 11559−11572.
(120) Clifford, D.; Donaldson, D. J. Direct Experimental Evidence for a Heterogeneous Reaction of Ozone with Bromide at the Air−Aqueous Interface. *J. Phys. Chem. A* **2007**, *111*, 9809−9814.
(121) Shultz, M. J.; Schnitzer, C.; Simonelli, D.; Baldelli, S. Sum Frequency Generation Spectroscopy of the Aqueous Interface: Ionic and Soluble Molecular Solutions. *Int. Rev. Phys. Chem.* **2000**, *19*, 123−153.
(122) Baldelli, S.; Schnitzer, C.; Shultz, M. J. The Structure of Water on HCl Solutions Studied with Sum Frequency Generation. *Chem. Phys. Lett.* **1999**, *302*, 157−163.
(123) Schnitzer, C.; Baldelli, S.; Shultz, M. J. Sum Frequency Generation of Water on NaCl, $NaNO_3$, $KHSO_4$, HCl, HNO_3, and H_2SO_4 Aqueous Solutions. *J. Phys. Chem. B* **2000**, *104*, 585−590.
(124) Liu, D.; Ma, G.; Levering, L. M.; Allen, H. C. Vibrational Spectroscopy of Aqueous Sodium Halide Solutions and Air−Liquid Interfaces: Observation of Increased Interfacial Depth. *J. Phys. Chem. B* **2004**, *108*, 2252−2260.
(125) Raymond, E. A.; Richmond, G. L. Probing the Molecular Structure and Bonding of the Surface of Aqueous Salt Solutions. *J. Phys. Chem. B* **2004**, *108*, 5051−5059.
(126) Tarbuck, T. L.; Ota, S. T.; Richmond, G. L. Spectroscopic Studies of Solvated Hydrogen and Hydroxide Ions at Aqueous Surfaces. *J. Am. Chem. Soc.* **2006**, *128*, 14519−14527.
(127) Levering, L. M.; Sierra-Hernández, M. R.; Allen, H. C. Observation of Hydronium Ions at the Air−Aqueous Acid Interface: Vibrational Spectroscopic Studies of Aqueous HCl, HBr, and HI. *J. Phys. Chem. C* **2007**, *111*, 8814−8826.
(128) Mucha, M.; Frigato, T.; Levering, L. M.; Allen, H. C.; Tobias, D. J.; Dang, L. X.; Jungwirth, P. Unified Molecular Picture of the Surfaces of Aqueous Acid, Base, and Salt Solutions. *J. Phys. Chem. B* **2005**, *109*, 7617−7623.
(129) Ishiyama, T.; Morita, A. Molecular Dynamics Analysis of Interfacial Structures and Sum Frequency Generation Spectra of Aqueous Hydrogen Halide Solutions. *J. Phys. Chem. A* **2007**, *111*, 9277−9285.
(130) Bian, H.-t.; Feng, R.-r.; Xu, Y.-y.; Guo, Y.; Wang, H.-f. Increased Interfacial Thickness of the NaF, NaCl and NaBr Salt Aqueous Solutions Probed with Non-Resonant Surface Second Harmonic Generation (SHG). *Phys. Chem. Chem. Phys.* **2008**, *10*, 4920−4931.
(131) Ghosal, S.; Brown, M. A.; Bluhm, H.; Krisch, M. J.; Salmeron, M.; Jungwirth, P.; Hemminger, J. C. Ion Partitioning at the Liquid/Vapor Interface of a Multicomponent Alkali Halide Solution: A Model for Aqueous Sea Salt Aerosols. *J. Phys. Chem. A* **2008**, *112*, 12378−12384.
(132) Brown, M. A.; D'Auria, R.; Kuo, I.-F. W.; Krisch, M. J.; Starr, D. E.; Bluhm, H.; Tobias, D. J.; Hemminger, J. C. Ion Spatial Distributions at the Liquid−Vapor Interface of Aqueous Potassium Fluoride solutions. *Phys. Chem. Chem. Phys.* **2008**, *10*, 4778−4784.
(133) Cheng, M. H.; Callahan, K. M.; Margarella, A. M.; Tobias, D. J.; Hemminger, J. C.; Bluhm, H.; Krisch, M. J. Ambient Pressure X-ray Photoelectron Spectroscopy and Molecular Dynamics Simulation Studies of Liquid/Vapor Interfaces of Aqueous NaCl, RbCl, and RbBr Solutions. *J. Phys. Chem. C* **2012**, *116*, 4545−4555.
(134) Brown, E. C.; Mucha, M.; Jungwirth, P.; Tobias, D. J. Structure and Vibrational Spectroscopy of Salt Water/Air Interfaces: Predictions from Classical Molecular Dynamics Simulations. *J. Phys. Chem. B* **2005**, *109*, 7934−7940.
(135) Salvador, P.; Curtis, J. E.; Tobias, D. J.; Jungwirth, P. Polarizability of the Nitrate Anion and Its Solvation at the Air/Water Interface. *Phys. Chem. Chem. Phys.* **2003**, *5*, 3752−3757.
(136) Gopalakrishnan, S.; Jungwirth, P.; Tobias, D. J.; Allen, H. C. Air−Liquid Interfaces of Aqueous Solutions Containing Ammonium and Sulfate: Spectroscopic and Molecular Dynamics Studies. *J. Phys. Chem. B* **2005**, *109*, 8861−8872.
(137) Dang, L. X.; Chang, T. M.; Roeselova, M.; Garrett, B. C.; Tobias, D. J. On NO_3−H_2O Interactions in Aqueous Solutions and at Interfaces. *J. Chem. Phys.* **2006**, *124*, 066101/1−066101/3.
(138) Thomas, J. L.; Roeselova, M.; Dang, L. X.; Tobias, D. J. Molecular Dynamics Simulations of the Solution−Air Interface of Aqueous Sodium Nitrate. *J. Phys. Chem. A* **2007**, *111*, 3091−3098.
(139) Molina, J. J.; Lectez, S.; Tazi, S.; Salanne, M.; Dufrêche, J.-F.; Roques, J.; Simoni, E.; Madden, P. A.; Turq, P. Ions in Solutions: Determining Their Polarizabilities from First-Principles. *J. Chem. Phys.* **2011**, *134*, 014511/1−014511/6.
(140) Brown, M. A.; Winter, B.; Faubel, M.; Hemminger, J. C. Spatial Distribution of Nitrate and Nitrite Anions at the Liquid/Vapor Interface of Aqueous Solutions. *J. Am. Chem. Soc.* **2009**, *131*, 8354−8355.
(141) Otten, D. E.; Petersen, P. B.; Saykally, R. J. Observation of Nitrate Ions at the Air/Water Interface by UV-Second Harmonic Generation. *Chem. Phys. Lett.* **2007**, *449*, 261−265.
(142) Jungwirth, P.; Curtis, J. E.; Tobias, D. J. Polarizability and Aqueous Solvation of the Sulfate Dianion. *Chem. Phys. Lett.* **2003**, *367*, 704−710.
(143) Tarbuck, T. L.; Richmond, G. L. Adsorption and Reaction of CO_2 and SO_2 at a Water Surface. *J. Am. Chem. Soc.* **2006**, *128*, 3256−3267.
(144) Du, H.; Liu, J.; Ozdemir, O.; Nguyen, A. V.; Miller, J. D. Molecular Features of the Air/Carbonate Solution Interface. *J. Colloid Interface Sci.* **2008**, *318*, 271−277.
(145) Hua, W.; Chen, X.; Allen, H. C. Phase-Sensitive Sum Frequency Revealing Accommodation of Bicarbonate Ions, and Charge Separation of Sodium and Carbonate Ions within the Air/Water Interface. *J. Phys. Chem. A* **2011**, *115*, 6233−6238.
(146) Charlson, R. J.; Lovelock, J. E.; Andrea, M. O.; Warren, S. G. Oceanic Phytoplankton, Atmospheric Sulfur, Cloud Albedo and Climate. *Nature* **1987**, *326*, 655−661.
(147) Schwartz, S. E. Are Global Cloud Albedo and Climate Controlled by Marine-Phytoplankton? *Nature* **1988**, *336*, 441−445.

(148) Berresheim, H.; Eisele, F. L.; Tanner, D. J.; McInnes, L. M.; Ramseybell, D. C.; Covert, D. S. 1993, Atmospheric Sulfur Chemistry and Cloud Condensation Nuclei (CCN) Concentrations over the Northeastern Pacific Coast. *J. Geophys. Res., Atmos.* **1993**, *98*, 12701−12711.
(149) Charlson, R. J.; Schwartz, S. E.; Hales, J. M.; Cess, R. D.; Coakley, J. A., Jr; Hansen, J. E.; Hofmann, D. J. Climate Forcing by Anthropogenic Aerosols. *Science* **1992**, *255*, 423−430.
(150) Kiehl, J. T.; Briegleb, B. P. The Relative Roles of Sulfate Aerosols and Greenhouse Gases in Climate Forcing. *Science* **1993**, *260*, 311−314.
(151) Tarbuck, T. L.; Richmond, G. L. Adsorption of Organosulfur Species at Aqueous Surfaces: Molecular Bonding and Orientation. *J. Phys. Chem. B* **2005**, *109*, 20868−20877.
(152) Allen, H. C.; Raymond, E. A.; Richmond, G. L. Surface Structural Studies of Methanesulfonic Acid at Air/Aqueous Solution Interfaces Using Vibrational Sum Frequency Spectroscopy. *J. Phys. Chem. A* **2001**, *105*, 1649−1655.
(153) Benjamin, I. Structure, Thermodynamics, and Dynamics of the Liquid/Vapor Interface of Water/Dimethylsulfoxide Mixtures. *J. Chem. Phys.* **1999**, *110*, 8070−8079.
(154) Chen, X.; Minofar, B.; Jungwirth, P.; Allen, H. C. Interfacial Molecular Organization at Aqueous Solution Surfaces of Atmospherically Relevant Dimethyl Sulfoxide and Methanesulfonic Acid Using Sum Frequency Spectroscopy and Molecular Dynamics Simulation. *J. Phys. Chem. B* **2010**, *114*, 15546−15553.
(155) Darvas, M.; Pojják, K.; Horvai, G.; Jedlovszky, P. Molecular Dynamics Simulation and Identification of the Truly Interfacial Molecules (ITIM) Analysis of the Liquid−Vapor Interface of Dimethyl Sulfoxide. *J. Chem. Phys.* **2010**, *132*, 134701/1−134701/11.
(156) Chen, X.; Allen, H. C. Water Structure at Aqueous Solution Surfaces of Atmospherically Relevant Dimethyl Sulfoxide and Methanesulfonic Acid Revealed by Phase-Sensitive Sum Frequency Spectroscopy. *J. Phys. Chem. B* **2010**, *114*, 14983−14988.
(157) Lopez, C. F.; Nielsen, S. O.; Klein, M. L.; Moore, P. B. Hydrogen Bonding Structure and Dynamics of Water at the Dimyristoylphosphatidylcholine Lipid Bilayer Surface from a Molecular Dynamics Simulation. *J. Phys. Chem. B* **2004**, *108*, 6603−6610.
(158) Watry, M. R.; Tarbuck, T. L.; Richmond, G. L. Vibrational Sum-Frequency Studies of a Series of Phospholipid Monolayers and the Associated Water Structure at the Vapor/Water Interface. *J. Phys. Chem. B* **2003**, *107*, 512−518.
(159) Viswanath, P.; Aroti, A.; Motschmann, H.; Leontidis, E. Vibrational Sum Frequency Generation Spectroscopic Investigation of the Interaction of Thiocyanate Ions with Zwitterionic Phospholipid Monolayers at the Air−Water Interface. *J. Phys. Chem. B* **2009**, *113*, 14816−14823.
(160) Sung, W.; Seok, S.; Kim, D.; Tian, C. S.; Shen, Y. R. Sum-Frequency Spectroscopic Study of Langmuir Monolayers of Lipids Having Oppositely Charged Headgroups. *Langmuir* **2010**, *26*, 18266−18272.
(161) Chen, X.; Hua, W.; Huang, Z.; Allen, H. C. Interfacial Water Structure Associated with Phospholipid Membranes Studied by Phase-Sensitive Vibrational Sum Frequency Generation Spectroscopy. *J. Am. Chem. Soc.* **2010**, *132*, 11336−11342.
(162) Nagata, Y.; Mukamel, S. Vibrational Sum-Frequency Generation Spectroscopy at the Water/Lipid Interface: Molecular Dynamics Simulation Study. *J. Am. Chem. Soc.* **2010**, *132*, 6434−6442.
(163) Mondal, J. A.; Nihonyanagi, S.; Yamaguchi, S.; Tahara, T. Three Distinct Water Structures at a Zwitterionic Lipid/Water Interface Revealed by Heterodyne-Detected Vibrational Sum Frequency Generation. *J. Am. Chem. Soc.* **2012**, *134*, 7842−7850.
(164) Chen, X.; Yang, T. L.; Kataoka, S.; Cremer, P. S. Specific Ion Effects on Interfacial Water Structure near Macromolecules. *J. Am. Chem. Soc.* **2007**, *129*, 12272−12279.
(165) Vlachy, N.; Jagoda-Cwiklik, B.; Vácha, R.; Touraud, D.; Jungwirth, P.; Kunz, W. Hofmeister Series and Specific Interactions of Charged Headgroups with Aqueous Ions. *Adv. Colloid Polym. Sci.* **2009**, *146*, 42−47.
(166) Lyklema, J. Simple Hofmeister Series. *Chem. Phys. Lett.* **2009**, *467*, 217−222.
(167) Kunz, W. Specific Ion Effects in Colloidal and Biological Systems. *Curr. Opin. Colloid Interface Sci.* **2010**, *15*, 34−39.
(168) Zhang, Y.; Cremer, P. S. Chemistry of Hofmeister Anions and Osmolytes. *Annu. Rev. Phys. Chem.* **2010**, *61*, 63−83.
(169) Johnson, C. M.; Tyrode, E.; Baldelli, S.; Rutland, M. W.; Leygraf, C. A Vibrational Sum Frequency Spectroscopy Study of the Liquid−Gas Interface of Acetic Acid−Water Mixtures: 1. Surface Speciation. *J. Phys. Chem. B* **2005**, *109*, 321−328.
(170) Minofar, B.; Jungwirth, P.; Das, M. R.; Manash, R.; Kunz, W.; Mahiuddin, S. Propensity of Formate, Acetate, Benzoate, and Phenolate for the Aqueous Solution/Vapor Interface: Surface Tension Measurements and Molecular Dynamics Simulations. *J. Phys. Chem. C* **2007**, *111*, 8242−8247.
(171) Mahiuddin, S.; Minofar, B.; Borah, J. M.; Jayanta, M.; Das, M. R.; Manash, R.; Jungwirth, P. Propensities of Oxalic, Citric, Succinic, and Maleic Acids for the Aqueous Solution/Vapour Interface: Surface Tension Measurements and Molecular Dynamics Simulations. *Chem. Phys. Lett.* **2008**, *462*, 217−221.
(172) Johnson, C. M.; Tyrode, E.; Kumpulainen, A.; Leygraf, C. Vibrational Sum Frequency Spectroscopy Study of the Liquid/Vapor Interface of Formic Acid/Water Solutions. *J. Phys. Chem. C* **2009**, *113*, 13209−13218.
(173) Rao, Y.; Subir, M.; McArthur, E. A.; Turro, N. J.; Eisenthal, K. B. Organic Ions at the Air/Water Interface. *Chem. Phys. Lett.* **2009**, *477*, 241−244.
(174) Casillas-Ituarte, N. N.; Chen, X.; Castada, H.; Allen, H. C. Na^+ and Ca^{2+} Effect on the Hydration and Orientation of the Phosphate Group of DPPC at Air−Water and Air−Hydrated Silica Interfaces. *J. Phys. Chem. B* **2010**, *114*, 9485−9495.
(175) Tang, C. Y.; Huang, Z.; Allen, H. C. Interfacial Water Structure and Effects of Mg^{2+} and Ca^{2+} Binding to the COOH Headgroup of a Palmitic Acid Monolayer Studied by Sum Frequency Spectroscopy. *J. Phys. Chem. B* **2011**, *115*, 34−40.
(176) Uosaki, K.; Noguchi, H.; Yamamoto, R.; Nihonyanagi, S. Interfacial Molecular Structures of Polyelectrolyte Brush in Contact with Dry Nitrogen, Water Vapor, Liquid Water, and Aqueous Electrolyte Solution Studied by Sum Frequency Generation Spectroscopy. *J. Am. Chem. Soc.* **2010**, *132*, 17271−17276.
(177) Kondo, T.; Gemmei-Ide, M.; Kitano, H.; Ohno, K.; Noguchi, H.; Uosaki, K. Sum Frequency Generation Study on the Structure of Water in the Vicinity of an Amphoteric Polymer Brush. *Colloid Surf., B* **2012**, *91*, 215−218.
(178) Kondo, T.; Nomura, K.; Murou, M.; Gemmei-Ide, M.; Kitano, H.; Noguchi, H.; Uosaki, K.; Ohno, K.; Saruwatari, Y. Structure of Water in the Vicinity of a Zwitterionic Polymer Brush as Examined by Sum Frequency Generation Method. *Colloid Surf., B* **2012**, *100*, 126−132.
(179) Chen, X.; Flores, S. C.; Lim, S.-M.; Zhang, Y.; Yang, T.; Kherb, J.; Cremer, P. S. Specific Anion Effects on Water Structure Adjacent to Protein Monolayers. *Langmuir* **2010**, *26*, 16447−16454.
(180) Tian, C. S.; Shen, Y. R. Structure and Charging of Hydrophobic Material/Water Interfaces Studied by Phase-Sensitive Sum-Frequency Vibrational Spectroscopy. *Proc. Natl. Acad. Sci. U.S.A.* **2009**, *106*, 15148−15153.
(181) Hopkins, A. J.; McFearin, C. L.; Richmond, G. L. SAMs under Water: The Impact of Ions on the Behavior of Water at Soft Hydrophobic Surfaces. *J. Phys. Chem. C* **2011**, *115*, 11192−11203.
(182) Brown, G. E., Jr.; Henrich, V. E.; Casey, W. H.; Clark, D. L.; Eggleston, C.; Felmy, A.; Goodman, D. W.; Grätzel, M.; Maciel, G.; McCarthy, M. I.; Nealson, K. H.; Sverjensky, D. A.; Toney, M. F.; Zachara, J. M. Metal Oxide Surfaces and Their Interactions with Aqueous Solutions and Microbial Organisms. *Chem. Rev.* **1999**, *99*, 77−174.
(183) Al-Abadleh, H. A.; Grassian, V. H. Oxide Surfaces as Environmental Interfaces. *Surf. Sci. Rep.* **2003**, *52*, 63−161.

(184) Grassian, V. H. Surface Science of Complex Environmental Interfaces: Oxide and Carbonate Surfaces in Dynamic Equilibrium with Water Vapor. *Surf. Sci.* **2008**, *602*, 2955−2962.
(185) Becraft, K. A.; Richmond, G. L. In Situ Vibrational Spectroscopic Studies of the CaF_2/H_2O Interface. *Langmuir* **2001**, *17*, 7721−7724.
(186) Hopkins, A. J.; Schrödle, S.; Richmond, G. L. Specific Ion Effects of Salt Solutions at the CaF_2/Water Interface. *Langmuir* **2010**, *26*, 10784−10790.
(187) Jubb, A. M.; Allen, H. C. Sulfate Adsorption at the Buried Fluorite−Solution Interface Revealed by Vibrational Sum Frequency Generation Spectroscopy. *J. Phys. Chem. C* **2012**, *116*, 9085−9091.
(188) Flörsheimer, M.; Kruse, K.; Polly, R.; Abdelmonem, A.; Schimmelpfennig, B.; Klenze, R.; Fanghänel, T. Hydration of Mineral Surfaces Probed at the Molecular Level. *Langmuir* **2008**, *24*, 13434−13439.
(189) Braunschweig, B.; Eissner, S.; Daum, W. Molecular Structure of a Mineral/Water Interface: Effects of Surface Nanoroughness of α-Al_2O_3 (0001). *J. Phys. Chem. C* **2008**, *112*, 1751−1754.
(190) Sung, J.; Zhang, L.; Tian, C.; Shen, Y. R.; Waychunas, G. A. Effect of pH on the Water/α-Al_2O_3 ($1\bar{1}02$) Interface Structure Studied by Sum-Frequency Vibrational Spectroscopy. *J. Phys. Chem. C* **2011**, *115*, 13887−13893.
(191) Ostroverkhov, V.; Waychunas, G. A.; Shen, Y. R. Vibrational Spectra of Water at Water/α-Quartz (0001) Interface. *Chem. Phys. Lett.* **2004**, *386*, 144−148.
(192) Yang, Z.; Li, Q. F.; Chou, K. C. Structures of Water Molecules at the Interfaces of Aqueous Salt Solutions and Silica: Cation Effects. *J. Phys. Chem. C* **2009**, *113*, 8201−8205.
(193) Jena, K. C.; Hore, D. K. Variation of Ionic Strength Reveals the Interfacial Water Structure at a Charged Mineral Surface. *J. Phys. Chem. C* **2009**, *113*, 15364−15372.
(194) Jena, K. C.; Covert, P. A.; Hore, D. K. The Effect of Salt on the Water Structure at a Charged Solid Surface: Differentiating Second- and Third-Order Nonlinear Contributions. *J. Phys. Chem. Lett.* **2011**, *2*, 1056−1061.
(195) Azam, M. S.; Weeraman, C. N.; Gibbs-Davis, J. M. Specific Cation Effects on the Bimodal Acid−Base Behavior of the Silica/Water Interface. *J. Phys. Chem. Lett.* **2012**, *3*, 1269−1274.
(196) Flores, S. C.; Kherb, J.; Konelick, N.; Chen, X.; Cremer, P. S. The Effects of Hofmeister Cations at Negatively Charged Hydrophilic Surfaces. *J. Phys. Chem. C* **2012**, *116*, 5730−5734.
(197) Flores, S. C.; Kherb, J.; Cremer, P. S. Direct and Reverse Hofmeister Effects on Interfacial Water Structure. *J. Phys. Chem. C* **2012**, *116*, 14408−14413.
(198) Kataoka, S.; Gurau, M. C.; Albertorio, F.; Holden, M. A.; Lim, S.-M.; Yang, R. D.; Cremer, P. S. Investigation of Water Structure at the TiO_2/Aqueous Interface. *Langmuir* **2004**, *20*, 1662−1666.
(199) Zhang, L.; Tian, C.; Waychunas, G. A.; Shen, Y. R. Structures and Charging of α-Alumina (0001)/Water Interfaces Studied by Sum-Frequency Vibrational Spectroscopy. *J. Am. Chem. Soc.* **2008**, *130*, 7686−7694.
(200) Arnolds, H.; Bonn, M. Ultrafast Surface Vibrational Dynamics. *Surf. Sci. Rep.* **2010**, *65*, 45−66.
(201) Ghosh, A.; Smits, M.; Bredenbeck, J.; Dijkhuizen, N.; Bonn, M. Femtosecond Time-Resolved and Two-Dimensional Vibrational Sum Frequency Spectroscopic Instrumentation to Study Structural Dynamics at Interfaces. *Rev. Sci. Instrum.* **2008**, *79*, 093907/1−093907/9.
(202) McGuire, J. A.; Shen, Y. R. Ultrafast Vibrational Dynamics at Water Interfaces. *Science* **2006**, *313*, 1945−1948.
(203) Smits, M.; Ghosh, A.; Sterrer, M.; Müller, M.; Bonn, M. Ultrafast Vibrational Energy Transfer between Surface and Bulk Water at the Air−Water Interface. *Phys. Rev. Lett.* **2007**, *98*, 098302/1−098302/4.
(204) Hsieh, C.-S.; Campen, R. K.; Vila Verde, A. C.; Bolhuis, P.; Nienhuys, H.-K.; Bonn, M. Ultrafast Reorientation of Dangling OH Groups at the Air−Water Interface Using Femtosecond Vibrational Spectroscopy. *Phys. Rev. Lett.* **2011**, *107*, 116102/1−116102/5.
(205) Ghosh, A.; Smits, M.; Bredenbeck, J.; Bonn, M. Membrane-Bound Water is Energetically Decoupled from Nearby Bulk Water: An Ultrafast Surface-Specific Investigation. *J. Am. Chem. Soc.* **2007**, *129*, 9608−9609.
(206) Bonn, M.; Bakker, H. J.; Ghosh, A.; Yamamoto, S.; Sovago, M.; Campen, R. K. Structural Inhomogeneity of Interfacial Water at Lipid Monolayers Revealed by Surface-Specific Vibrational Pump−Probe Spectroscopy. *J. Am. Chem. Soc.* **2010**, *132*, 14971−14978.
(207) Eftekhari-Bafrooei, A.; Borguet, E. Effect of Surface Charge on the Vibrational Dynamics of Interfacial Water. *J. Am. Chem. Soc.* **2009**, *131*, 12034−12035.
(208) Eftekhari-Bafrooei, A.; Borguet, E. Effect of Hydrogen-Bond Strength on the Vibrational Relaxation of Interfacial Water. *J. Am. Chem. Soc.* **2010**, *132*, 3756−3761.
(209) Eftekhari-Bafrooei, A.; Borguet, E. Effect of Electric Fields on the Ultrafast Vibrational Relaxation of Water at a Charged Solid−Liquid Interface as Probed by Vibrational Sum Frequency Generation. *J. Phys. Chem. Lett.* **2011**, *2*, 1353−1358.
(210) Bredenbeck, J.; Ghosh, A.; Nienhuys, H.-K.; Bonn, M. Interface-Specific Ultrafast Two-Dimensional Vibrational Spectroscopy. *Acc. Chem. Res.* **2009**, *42*, 1332−1342.
(211) Xiong, W.; Laaser, J. E.; Mehlenbacher, R. D.; Zanni, M. T. Adding a Dimension to the Infrared Spectra of Interfaces Using Heterodyne Detected 2D Sum-Frequency Generation (HD 2D SFG) Spectroscopy. *Proc. Natl. Acad. Sci. U.S.A.* **2011**, *108*, 20902−20907.
(212) Zhang, Z.; Piatkowski, L.; Bakker, H. J.; Bonn, M. Interfacial Water Structure Revealed by Ultrafast Two-Dimensional Surface Vibrational Spectroscopy. *J. Chem. Phys.* **2011**, *135*, 021101/1−021101/3.
(213) Zhang, Z.; Piatkowski, L.; Bakker, H. J.; Bonn, M. Ultrafast Vibrational Energy Transfer at the Water/Air Interface Revealed by Two-Dimensional Surface Vibrational Spectroscopy. *Nat. Chem.* **2011**, *3*, 888−893.
(214) Isaienko, O.; Borguet, E. Ultra-Broadband Sum-Frequency Vibrational Spectrometer of Aqueous Interfaces Based on a Non-Collinear Optical Parametric Amplifier. *Opt. Express* **2012**, *20*, 547−561.